ABSTRACT

EVALUATING HYDROLOGIC RESPONSE OF SATELLITE PRECIPITATION IN A SEMI-ARID WATERSHED

By

Marwan M. A. Kheimi

August 2013

Rainfall estimation from satellite observations has uncertainties and inconsistency at different locations and so four different satellite products were selected for validation in Saudi Arabia. The satellite products selected for this study are TRMM, PERSIANN, CMORPH, and GSMap-MVK which are compared with gauge observed rainfall data using conventional statistical methods at daily, 10-daily, and monthly time scale. The validation results show that all the products can predict rainfall in the study area reasonably well but overestimates rainfall in the regions. However, this bias is comparatively less in the semi-arid part of the country where most of the rain falls. Therefore, all the four satellite products were used in SWAT model to study the hydrologic response in a semi-arid watershed located in the western part of the country. Results show that simulation from TRMM rainfall estimates agrees better with that of gauge observations at daily time scale.

EVALUATING HYDROLOGIC RESPONSE OF SATELLITE PRECIPITATION IN A SEMI-ARID WATERSHED

A THESIS

Presented to the Department of Civil Engineering and Construction Engineering Management

California State University, Long Beach

In Partial Fulfillment

of the Requirements for the Degree

Master of Science in Civil Engineering

Committee Members:

Rebeka Sultana, Ph.D. (Chair)
Kuolin Hsu, Ph.D.
Pitiporn Asvapathanagul Ph.D.

College Designee:

Burkhard Englert, Ph.D.

By Marwan M. A. Kheimi

B.S., 2009, Umm Al-Qura University, Makkah

August 2013

ACKNOWLEDGEMENTS

I would like to thank my advisor, Dr. Rebeka Sultana, for her guidance and support throughout this entire thesis. I would also like to thank Dr. Kuolin Hsu, Associate Professor, at University of California-Irvine and Dr. Pitiporn Asvapathanagul at California State University, Long Beach for serving on my committee. Sincere thanks goes to past and current members of the Presidency of Metrological and Environment (PME) for providing data, insight, and valuable discussion related to my research. In addition, I would like to thank Ph.D. student. Muhammad Felemban at Purdue University, West Lafayette and Master's student Fiasal Al-Dossari at Rochester Institute of Technology, New York for their assistance with computer programming and other computer-related issues. I also, appreciate the huge endorsement and the financial aid from the government of Saudi Arabia represented by the Saudi Arabia Cultural of Mission (SACM). Lastly, I want to thank my family and friends for their support throughout these years as I pursued a Master's degree in Civil Engineering.

TABLE OF CONTENTS

LIST OF TABLES

LIST OF FIGURES

FIGURE Page

FIGURE Page

CHAPTER 1

INTRODUCTION

1.1 Motivation and Problem Statement

Water resource is an indispensable commodity for every human being and every living creature in the ecosystem. The water environment characterized in the hydrological cycle including flooding, drought, and all of its crucial and beneficial forms are playing a significant role in economy, health, urbanization, and environment. Scarcity of water supplies, rainfall, surface runoff, and aquifer recharge will seriously influence the social survival and the welfare of communities. On the other hand, floods make an enormous impact on the environment and society. Floods destroy drainage systems in cities, causing raw sewage to spill out into bodies of water. In addition, in cases of severe floods, buildings can be significantly damaged and even destroyed. This can lead to catastrophic effects on the environment as many toxic materials such as paint, pesticide, and gasoline can be released into the rivers, lakes, bays, and ocean, killing maritime life.

The human, construction, commercial, transportation, education, health, and industrial activities will be negatively disrupted. This will lead to serious impacts on social and economic development and progress of a country, national economies would be adversely affected not only by the direct impacts of climate change, but also through the cost of adaptive measures and the knock-on implications of changes elsewhere.

Therefore, rainfall measurements are important meteorological data. Rainfall rate and quantity interact with many other factors to influence erosion, vegetative cover, groundwater recharge, stream water chemistry, and runoff of non-point source pollution into streams. Weather and atmospheric researches rely on the conventional rainfall measuring instruments that observe and monitor precipitation and its other forms. Conventional rain gauges are categorized into recording and non-recording gauges. The latter rain gauge objective is to measure the volume or weight of precipitation collected in a vessel. Either the readings could be taking manually or remotely whichever the rain gauge is occupied with. The rainfall data from the rain gauges needs to be monitored regularly and recorded. The proper functioning of the rain gauges needs to be ensured through the field visit by the federation staff and the maintenance visit by the staff of the supplier. Regular systems of checks and balances are required by verifying the data of adjacent rain gauges and checking with the data of the nearest Meteorological Department rain gauge.

The reading is susceptible to natural and non-natural influences that may lead to errors in the reading. The most significant influences on the accuracy of precipitation measurement are the environment and wind at the installation site rather than the performance of the instrument itself. (Japan Meteorological Agency 2007) The environment of the instrument's location significantly influences observation of precipitation and therefore, the surroundings of the observation site must be considered before final installation of the gauge. Other limitation and errors can occur from windshield error, wetting error, heavy rain, evaporation error, and instrument accuracy error.

Although, the point measurement have high accuracy, ground-based precipitation network like United States is not common in most parts of the globe. Therefore, it limits the development and use of hydrologic models to monitor and warn for flood or droughts for decision-making systems (AghaKouchak et al. 2011) in those regions. Therefore, satellite precipitation is increasingly in demand to provide rainfall information at a spatial scale of interest. Some of the satellite data are now available and accessible in near–real time with almost global coverage over the oceans and parts of the world where conventional ground-based observations (rain gauges and radars) are very sparse or nonexistent (Dinku et al. 2009). Further, with continuous improvement in sensor technology and new methods in merging various data sources, the satellite precipitation data are now available at high measurement accuracy at sub-daily temporal scale (Thiemig et al. 2012).

In this study is focusing on considering modern new approaches with global coverage remotely sensed satellite precipitation products. With high special resolution and global coverage resulted in an alternative source of rainfall data for hydrological applications. One of the main targets in studying the hydrological and environmental characteristics of any area is to identify the major factors affecting the magnitude and distribution of climate parameters, such as rainfall, air mass movement, the distance from the source of moisture, and topography of watersheds. In arid and extremely arid regions, the magnitude and distribution of these parameters vary spatially and temporally affecting the hydrological cycle of the area. Description and prediction of the rainfall variability in space and/or in time are fundamental requirements for a wide variety of human activities and water project designs.

In Saudi Arabia, there are only 29 conventional rain gauges installed across the country (FIGURE 1). Highest number of rain gauges is seen in the eastern province (Al-Sharqiah) although they are not uniformly spread over the area. However, the western part of the country, which has seen several devastating flash, flood events (e.g., on November 25, 2009 at Jeddah and May 5, 2010 at Riyadh, among many others) in recent years, have of less than 5 rain gauges (Almazroui 2011). Consequently, magnitude of the rainfalls in the impacted area could not be assessed with desired accuracy. Thus, for Saudi Arabia, satellite derived precipitation data can be a suitable alternative to rain gauges.

However, the satellite- retrieved estimates can be an overestimation or underestimation of the actual rainfall amount, which could lead to uncertainty in the operational decision-making. The difference in data products is mainly because each satellite product uses different algorithm and different spectra of the wavelengths to produce precipitation data. Further, accuracy of these estimates also varies over different regions of the world.

Consequently, an in depth validation of a satellite product is necessary before using the data with confidence in decision support systems or in hydrologic models. The motivation of this thesis is to assess several satellite products against ground observation over the Saudi Arabia region to find out which product best describes the regional climate dynamics and later can be used in hydrologic models or climate models. The study area (Saudi Arabia) is a special case due to its geographic location and arid, dry atmosphere. The remote-sensing precipitation data with high agreement with observation will play an

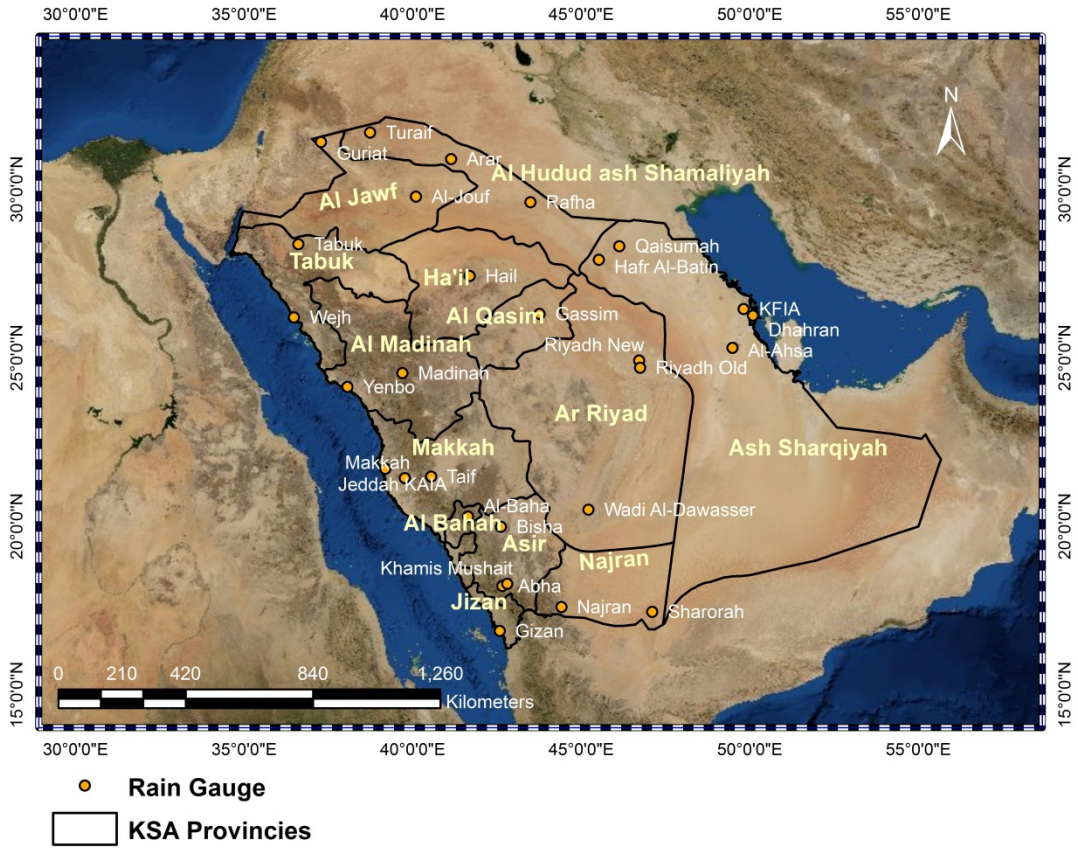

FIGURE 1. Location map of the rainfall gauge recording stations.

important role in preparing flood map or future flood forecasting using hydrologic models or climate forecasting using climate models.

1.2 Literature Review

Several satellite precipitation products are available with near global coverage and high temporal resolution. These products can have as short as 3-hourly to as long as daily temporal resolution. For this study, four satellite precipitation products in TABLE 1 has been chosen, Precipitation Estimation from Remotely Sensed Information using Artificial Neural Networks (PERSIANN), Precipitation Estimation from Global Satellite Mapping of Precipitation (GSMaP) project, product called as Global Satellite Mapping of

Precipitation Microwave-IR Combined Product (GSMaP_MVK V.5.2221), Tropical Rainfall Measurement Monitoring (TRMM), and National Oceanic and Atmospheric Administration, Climate Prediction Center (NOAA,CPC) Morphing Technique (CMORPH) precipitation products has been selected because they have finer spatial resolution. Course resolution product cannot capture all the local dynamics and so a finer resolution product is always highly regarded as best alternative for conventional rain gauge. TABLE 1 lists some of the precipitation products information.

From TABLE 1 summarization of different climates and regions from the world of the performance of remotely sensed precipitation estimation products. In a study prepared by Dinku et al. (2009) PERSIANN and CMORPH products have been investigated its accuracy over the region of South America, Colombia. The validation was done for whole as well as different parts of the country. The validation results of in comparison between the two products indicates that PERSIANN has a serious overestimation while CMORPH exhibited the best performance among the products investigated. Moreover, Novella and Thiaw (2008) precipitation data was better than PERSIANN and TRMM products to detect rain versus non-rain events against rain gauges. In another study performed by AghaKouchak et al. (2011) across the central United States to evaluate the satellite-retrieved extreme precipitation it found that CMORPH and PERSIANN products data sets lead to better estimates than TAMPA-RT, and TAMPA-V6. In addition, Sohn et al. (2010) arrived to the same conclusion regarding the better agreement with observation in the Korean Peninsula region. Thiemig et al. (2012) concluded that CMORPH showed specific strength in rainfall estimating over mountainous area under sparse conditions and TRMM 3b42 succeeded in detecting

TABLE 1. Studies on Performance of Satellite Rainfall Products Estimates

Location	Climate and Topography	Study Period	Study Area (km^2)	Results	Products Used in Study	Annual Rainfall (mm)	No. of Stations	Author and year of publication
South America, Colombia	Complex terrain with mountain range and partially Amazon vast plain	2003-2005	1.142 million	PERSIANN and GSMaP-MVK (↓) with significant over estimation and under estimation respectively; CMORPH and GSMaP-MVK + showed (↑)	PERSIANN, GSMaP-MVK, GSMaP+, and CMORPH	500 to 4,000	600	Dinku et al. 2009
Europe, Greece	Mediterranean climate; chain of mountains from northwest to southwest; islands and plain areas	1998-2006	131,940	TRMM 3b43(↑) but TRMM 3b42 and CMAP showed (-)	TRMM 3b43, 3b42, 3A12, GPCP-1DD, GPCP-CPC, and CMAP	400 to 1,500	76	Feidas et al. 2009

TABLE 1. Continued

Location	Climate and Topography	Study Period	Study Area (km^2)	Results	Products Used in Study	Annual Rainfall (mm)	No. of Stations	Author and year of publication
Mali, Senegal, and Burkina Faso	Arid to semi-arid	June to September of 2008	1.24 million (Mali), 196,723 (Senegal), and 274,000 (Burkina Faso)	RFE, ARC, and CPC unified showed (↑) while PERSIANN, TAMASAT, and TRMM (↓)	RFE, ARC, TRMM 3b42-RT, CMORPH, PERSIANN, TAMST, and CPC unified gauge	50 to 100	133	Novella and Thiaw 2008
Zambezi, Volta, Juba-Shabelle, and Baro-Akobo river basins	Arid to semi-arid	2003-2006	1.35 million	GFROF 6.0 and GSMaP-MVK (↓), while RFE 2.0 and TRMM 3b42 (↑)	CMORPH, RFE 2.0, TRMM 3b42 , GPROF 6.0, PERSIANN, and GSMaP-MVK	700 to 1,500	205	Theimig et al. 2012
China Three Gorges	Complex terrain; mountainous region	1998-2009	NA	TAMPA (↑)	TRMM TMPA	900 to 1,400	34	Zhao and Shepherd 2012

TABLE 1. Continued

Location	Climate and Topography	Study Period	Study Area (km^2)	Results	Products Used in Study	Annual Rainfall (mm)	No. of Stations	Author and year of publication
USA, Texas, Oklahoma, Kansas, Nebraska, Iowa, Missouri, Arkansas, and Louisiana	Humid continental and sub-humid subtropical to semi-arid steppe climate	2005-2008	NA	CMORPH and PERSIANN (↑), however TAMPA-TR and TMPA-V6 (↓)	CMORPH, PERSIANN, TMPA-RT, and TMPA-V6	450 to 1,300	Radar estimates and rain gauge	AghaKouchak et al. 2011
Korean Peninsula	Mountainous region, affected by Asian monsoon and relatively warm and wet	2003-2006	220,847	PERSIANN, NRL blended, TMPA (↓), while CMORPH (↑)	TRMM TMPA, CMORPH, PERSIANN, and NRL	NA	520	Sohn et al. 2010

Note: (↑) indicates better agreement with ground observations; (↓) shows poor performance; (-) shows balanced performance; N/A not available.

seasonal variability and timing of rainfall events in the African region while Feidas et al. (2009) in Greece the TRMM 3b42 showed reasonable skill with detecting rainfall. Therefore, in this study, the selected satellite products will be evaluated to identify specific weaknesses and strengths of respective products using traditional statistical

TABLE 2. Summary of High-Resolution Precipitation Products Selected in This Study

Precipitation Product	Algorithm Used	Launched Since	Spatial Resolution	Spatial Coverage	Temporal Resolution	References
TRMM3B42	Version 7 TRMM Multi-Satellite Precipitation Analysis	1997	0.25° X 0.25°	50°N-50°S	3 hrs.	Huffman et al. 2007
PERSIANN	Neural Network Function Classification/ Approximation Procedures	1997	0.25° X 0.25°	60°N-60°S	30 min.	Sorooshian et al. 2000
GSMaP-MVK Ver.5.222	Combination of TRMM TMI, Aqua AMS R-E, DMSP SSM/I and SSMIS, NOAA AMS U-A/B and MHS, MetOp, AMS U-A and MHS, and Geostationary Infrared (IR) imagers as inputs	2000	0.1° X 0.1°	60°N-60°S	1 hr.	Okamoto et al. 2007
CMORPH	CPC MORPHing technique	1997	0.25° X 0.25°	60°N-60°S	30 min.	Joyce et al. 2004

method of analysis. Furthermore, there has been very limited studies on assessing satellite products over Saudi Arabia and thus raises the need for the validation of these products as an alternative for conventional rain gauge

Recently, with the rapid change of algorithms and computational capabilities an increasing number of models have been released such as SAC-SMA, DHSVM, HSPF, and MIKE-SHE. Basically, runoff models can be divided into two types of models: Physical and nonphysical analysis models. Physical models deals with the kinetic processes that occur in the watershed such as rainfall, temperature, wind speed, humidity, and solar radiation etc. On the other hand, the non-physical models concerns with the relationship between the data in location and different time without looking into the physical process occurring in the watershed.

In this study Soil and Water Analysis Tool (SWAT), a physical-based model, was used. Hence, the general theoretical considerations of nutrient processes are necessarily to be reviewed. SWAT theory can be fundamentally found in the SWAT Theory (Neitsch et al. 2002), brief explanations were implemented in the following sections as the basic background of the model configuration.

1.2.1 Sacramento Soil Moisture Accounting Model (SAC-SMA):

The model is a conceptually based rainfall runoff model with spatially lumped parameters. Development of the model involves generating river estimates on basins with a response time of greater than 12 hours. The model uses mean precipitation, evaporation, and air temperature as input to calculate estimated discharge. The model is ideal for river basins ranging from 100 to 1,500 square miles in size, except the outside of

this range. Basin sizes differ according to geomorphology, hydrologic region, estimate point requirements, and availability of the data. The SAC-SMA model parameters can be manually and automatically calibrated to make the model simulation match the historical data recorded from the interested study area**.**

1.2.2 Hydrologic Simulation Program-FORTRAN (HSPF):

HSPF is defined as physical based model. The model has three main components (viz. PERLND, IMPLND, and RCHRES) that help simulating pervious land segments, impervious areas, and free-flow reaches/mixed reservoirs. HSPF uses a Storage Routing technique to track water from one reach to the next throughout stream processing. In the model, the amount of water available in the soil and on the land surface for evapotranspiration ET and real (ET) is a function of the potential ET (user input) mandate. In addition, there is no plant-growth module, density, root growth, effect of vegetation type, and stage change along with the lower zone storage, the moisture of the soil layer is taken into the parameter that controls actual ET (Singh et al. 2005). There is no grid flow component in the HSPF. However, in the lower and upper zone storage there is no control of the efficient water removal effect from the field due totaling is endured in the parameters that control.

1.2.3 Distributed Hydrology Soil Vegetation Model (DHSVM):

DHSVM provides a dynamic representation of watershed process at the spatial scale described by Digital Elevation Model (DEM) data (typically 10-90 m horizontal resolution). This characterization of topography is used to model topographic controls on absorbed shortwave radiation, precipitation, air temperature, and downslope. Individual

grid cells are hierologically linked through the surface and subsurface flow routing (Singh and Frevert 2002). Typically, the model is applied at high spatial resolutions on the order of 100 m for watersheds of up to 104 km² and at sub-daily spans for multi-year simulations. It has been applied mostly to mountainous watersheds in the Pacific Northwest in the United States.

1.2.4 MIKE-SHE:

The MIKE-SHE is a model that has the capability of simulating surface and ground water movement, and their interactions, and points the associated point non-point source water quality concern. There is no limitation regarding the area of the studied watershed chosen. The system has no limitations regarding watershed size. Also, simulates different types of water control structures as well as water use and management operations, including irrigation systems, pumping wells, and other structures (Yan and Zhuang 2001). Using many of the DHI add-on modules, the user can further investigate a variety of agricultural practices and environmental protection alternatives. The results can be presented in a built-in graphic and digital post-processor model calibration and assessment of current conditions and management. An animated model scenario is another addition for analyzing and presenting results.

1.2.5 Soil and Water Analysis Tool (SWAT):

SWAT is a physical hydrologic/water quality model developed by United States Department of Agriculture-Agricultural Research Service (USDA-ARS), a successor of EPIC and SWRRB. It is a nonstop time model that operates on a daily time, and sub-daily step. The main goal of developing the model is to forecast the impact of

management on water, sediment, and agricultural chemical yields in large ungauged basins (Hao et al. 2003).

To satisfy the objective, the model:

SWAT is physically based model (calibration is possible on ungauged basins).

Uses readily available inputs such as: precipitation, temperature, humidity, wind speed, and solar radiation, land cover/land use, soil cover, etc.

Efficiently computable to operate on large basins in a reasonable time.

Continuum in time and capable of simulating long periods for computing the effects of management changes.

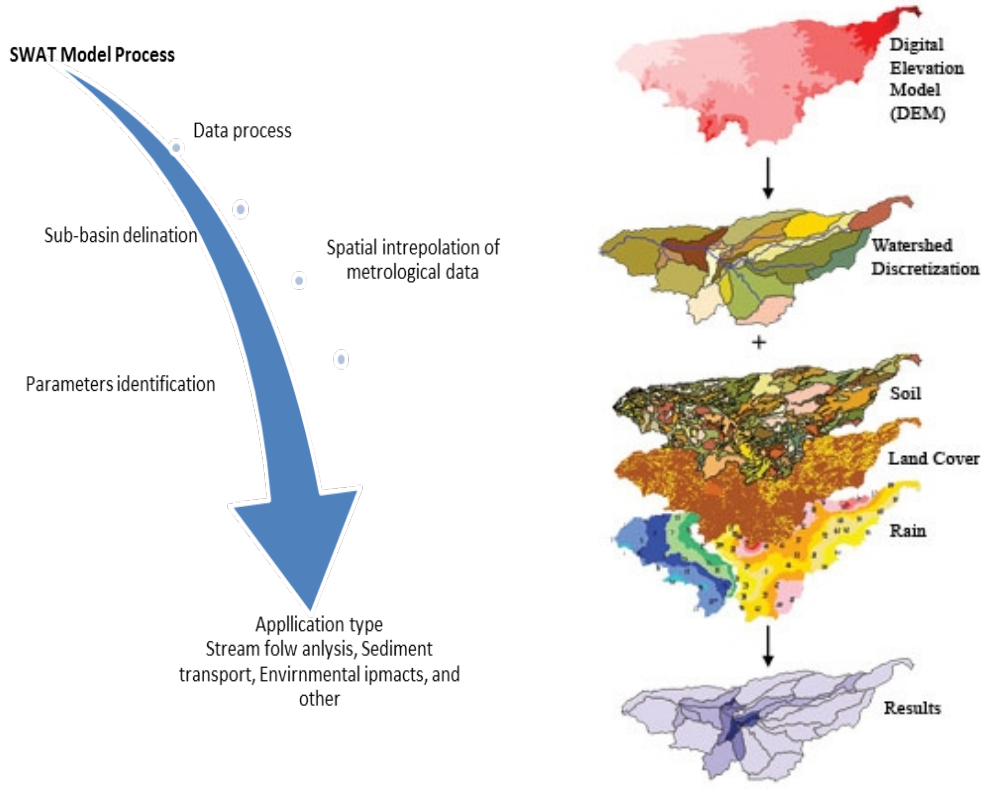

FIGURE 2. SWAT input layers and results manifestation retrieved from AGWA.

Benefits of using this model rather than other models:

Watersheds with no monitoring stream gauges can be modeled.

The relative impact of alternative input data such as changes in management practices, climate, vegetation, etc. that has an impact on water quality or other variables of interest can be quantified.

There have been concerns regarding the ability of satellite-based precipitation products to accurately capture rainfall amounts overland. The paper summarizes a methodology that adjusts satellite products utilizing ground-based precipitation data over seven basins around the continental U.S. (Tobin and Bennet 2012). The paper methodology is not a simple bias adjustment, but a three-step process transforms a satellite-based or rain gauge data. The approach has been implemented on seven moderate-to-large size watersheds. In another study by Bitew et al. (2012) in Ethiopia, used multiple satellite-based precipitation products and simulating streamflow in SWAT model. The predicative ability of each satellite rainfall was examined and calibrated in two different approaches with rain gauge input and satellite rainfall estimations.

1.3 Objective

The scope of the study will focus on the following points:

Collection of hydro-metrological data from the National Oceanic and Atmospheric Administration (NOAA) and locally from Presidency of Metrology and Environment (PME).

Retrieval of physical data from satellite images such as, land cover/land use, digital elevation model (DEM) and soil cover.

TABLE 3. Studies on Performance of Satellite Rainfall Products for Hydrologic Simulation

Location	Author and Year of Publication	Climate and Topography	Study Area (km^2)	Simulated Parameters	NS and R^2 for Stream Flow on Monthly Basis	Satellite Rainfall Product
1) San Pedro, AZ	Tobin and Bennett 2012	Dry and humid climatic settings	1) 1,971	Stream Flow	NS = 0.96, R^2 = 0.88	TRMM CMORPH
2) Cimarron, OK			2) 3,110		NS = 0.90	
3) mid-Rio Grande, TX			3) 7,720		NS = 0.91	
4) Yocano, MS			4) 8,905		NS = 0.62	
5) Alapaha, AR			5) 3,596		NS = 0.71	
6) mid-Nueces, NC			6) 2,477			
and 7) Upper Tar, NC			7) 619		NS = 0.52	
(USA)						
Blue Nile River (Ethiopia)	Bitew et al. 2012	Humid, semi-arid and arid regions	299	Stream Flow	R^2 = 0.83	CMORPH
					R^2 = 0.83	TRMM 3B42RT
					R^2 = 0.54	TRMM 3B42
					R^2 = 0.72	PERSIANN

Simulate the runoff across the basin.

Validation and calibration of runoff output from the model was not completed, due to non-availability of stream gauges.

1.4 Thesis Outline

In Chapter 2, precipitation products, PERSIANN, TRMM, GSMaP_MVK, and CMORPH are discussed in detail. The chapter also includes discussion of the statistical methods used for analyzing the satellite data and methods to compare SWAT simulated runoff. The validation results of satellite precipitation are discussed and analyzed in Chapter 3. In Chapter 4, the input data required for hydrologic model is discussed along with the analysis of results of simulated runoff. Finally, Chapter 5 includes summary from the results and conclusion of the study.

CHAPTER 2

DATA AND METHODOLOGY

2.1 Study Area

Satellite data were validated against rain gauges over the entire country of Saudi Arabia, which is located in the Southwest of Asia (Wikipedia 2013, "Geography of Saudi Arabia"). It covers one third of the Arabian Peninsula and it links Asia with Africa (Subyani et al., 2010; Wikipedia 2013, "Geography of Saudi Arabia"). It is located in the sub-tropical belt and is bounded by latitudes 12°N and 35°N and longitudes 30°W and 57°W (FIGURE 1). Geography of Saudi Arabia is dominated by the Arabian Desert and its largest desert, known as the Empty Quarter (locally called "Rub' al Khali"), occupies 647,000 km^2 of the Southern part of the country(Wikipedia 2013, "Saudi Arabia: Geography"). There are no rivers or lakes in the country, but wadis are numerous (Wikipedia 2013, "Saudi Arabia: Geography"). Nouh (2006) defined "wadis" as streams, which run full for short time after a heavy rainfall. Southwest of the country is more mountainous and the two mountain ranges, the Hijaz to the north and the Asir farther south, lies along the western coast (Wikipedia 2013, "Hijaz mountains"). Topography also plays an important role in the country's climate. Most part of the study area is arid and have desert climate (Koppen and Geiger 1928; Abdullah and Al-Mazroui 1998) but southwest is semi-arid. This exception in the climatology of the southwest can be explained by the role of mountains and air masses that proceed from different directions

over the country during the year. During winter (December-February), the Mediterranean cyclones migrate from west to east in association with upper troughs and active phases of subtropical and polar jets (Abdullah and Al-Mazroui 1998). This front further picks up more moisture from the Red sea (Subyani et al. 2010). However, its potential decreases from north to south except for the mountainous south-west region, where the topographic effects of Hijaz escarpments modify air mass. Orographic effect is the main cause of rainfall during this period. During the summer season (June-August) the circulation pattern is altered (Abdullah and Al-Mazroui 1998). Monsoonal air mass from Indian Ocean is predominant, creating thunderstorms along the escarpment and the southern part of the Red Sea coast (Subyani 2004). Nevertheless, northern part of the country remains dry because cold air mass adverts from the Atlantic Ocean (Abdullah and Al-Mazroui 1998). Moist southeasterly monsoon air causes rain during spring (March-May) as inter-tropical front move northwards. This rainfall is mainly along the leeward side of the mountains and the Red Sea coast (Subyani 2004). This southeasterly air weakens because of increasing northern westerly air front during Autumn (September-November). With a strong convergence of two fronts, tropical phenomenon rises and widespread rainfall occurs along the mountains of the southwest and the Red Sea coast. Thus, southwest of the country represents a unique climate. It receives more rain than any other part of the country and characterized by precipitation events throughout the year (Almazroui 2011). Rainfall in the rest of the country that generally falls from October through April is scarce, irregular and unreliable (Ministry of Agriculture and Water, 1984). FIGURE 3 shows the temporal and spatial distribution of rainfall using rain data from 1985 to 2005 in different parts of Saudi Arabia. Annual average rainfall in

the southwest is about 200 mm (see FIGURE 3) while most of the rain falls during spring season. The duration of rainfall is usually short but can consist of one or two high-intensity thunderstorms (Almazroui, 2011). Duration, intensity, and return periods of rainfalls affects wadis which bring in surface runoff from high elevated lands to low level coastal areas (Subyani, 2011). Nevertheless, the desert soil of Saudi Arabia does not soak water easily and thus, even a small storm can cause flash flood.

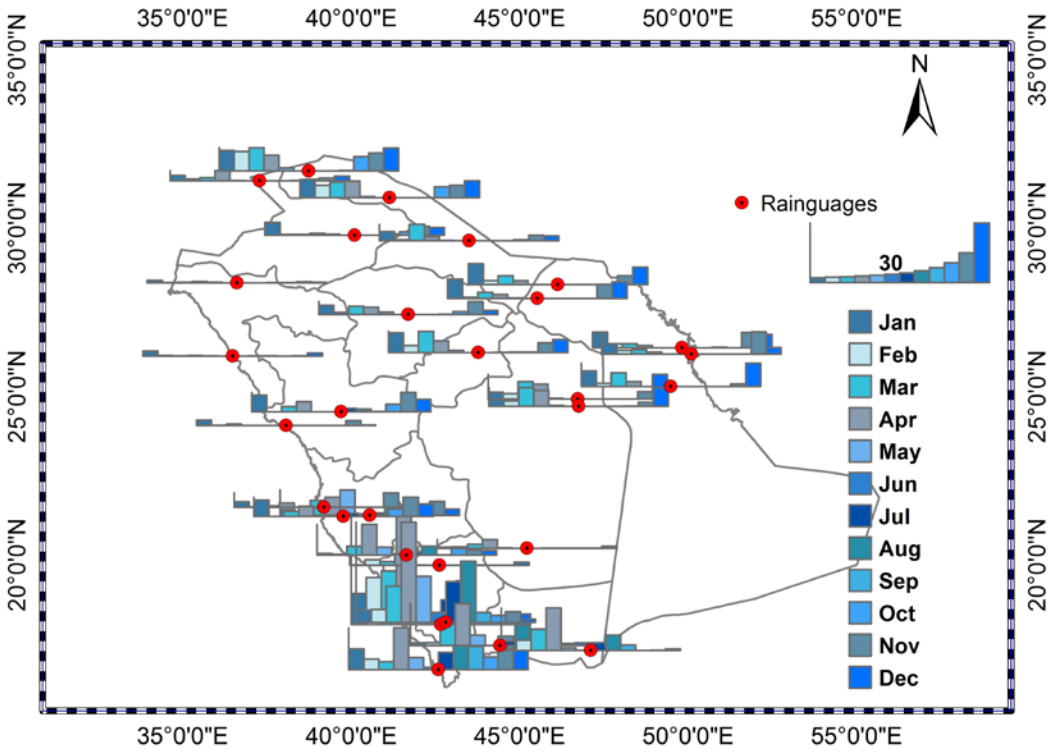

FIGURE 3. The average monthly precipitation events from 1985–2005 over the major cities in Saudi Arabia.

To study hydrologic response of rainfall, a watershed is selected in Jeddah City (Makkah Province) which is affected by recent flash floods. The watershed is centered at 39°19'55.8"E 21°31'16.7"N and is shown in FIGURE 4. It encompasses flood plain of a

group of wadies to eastern side of the city. The high mountains lie right to the basin with 711 m summit within the studied area. This watershed is categorized as urbanized area and semi-arid area. In 2009, the city was exposed to a devastating flood from one of the eastern wadi, which is referred to as Wadi Qows. Recently, this area has been affiliated with flash floods due to intense rainfall, accumulated sediments from the wadi, and lack of urban drainage system that can withhold huge amount of rainfall. The area of the basin is 124.095 km², length of 27 km, the highest elevation is 2,346 m while the average elevation is 182 m, mean slope 19.3%, and comprises of 13 sub-basins. The watershed was delineated from 30 arc second (100 m) grid resolution Digital Elevation Model data from USGS for Jeddah City.

2.2 Station Data

Meteorological data were collected from Presidency of Meteorology and Environment (PME) of Saudi Arabia. There are only 29 gauging stations across the country. The stations have continuous daily data on rainfall, temperature, relative humidity, wind speed and some of them stated collected weather data as early as 1970. Automated sensors are used to collect the weather data. The data was manually checked for consistency and accuracy. Spatial distribution of the observation stations are shown in FIGURE 5. The gauges are installed at various elevations. Station "Gizan" along the Coast of Read Sea is at 7.2 mm while station "Abha" has the highest elevation (2,093.4 m) and at the south-west of the country. The rainfall data from the ground observation stations was used to validate the satellite data. Other meteorological data was used for hydrologic modeling. There is no stream gauging station within the country. Therefore, the model-generated streamflow was studied at the watershed outlet.

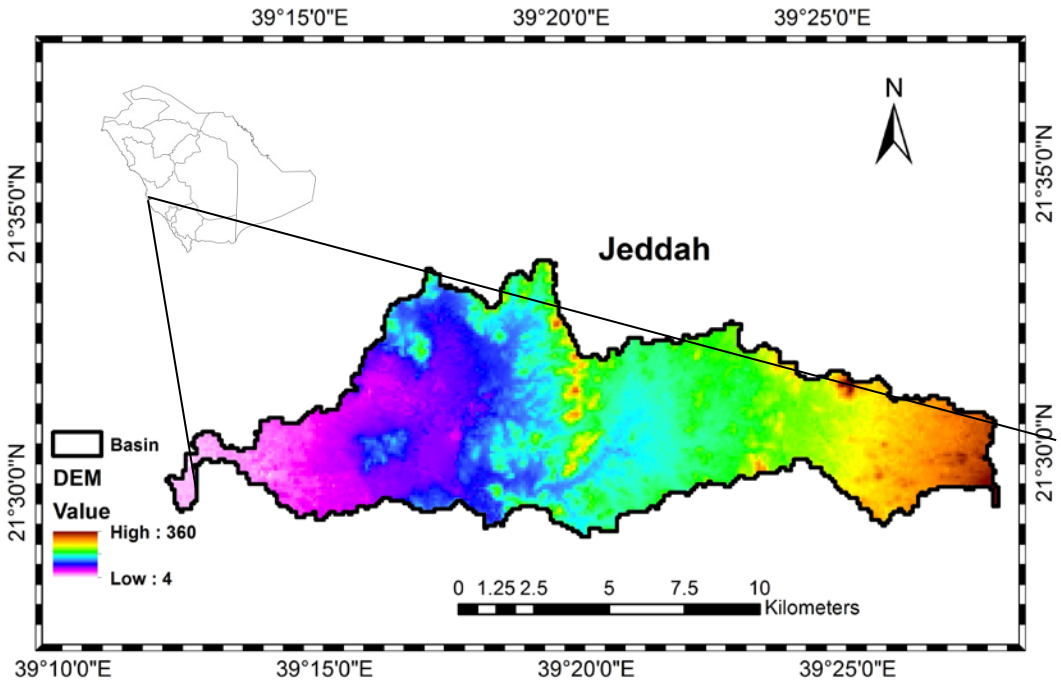

FIGURE 4. Location and boundary of watershed in Makkah Province used for hydrologic study.

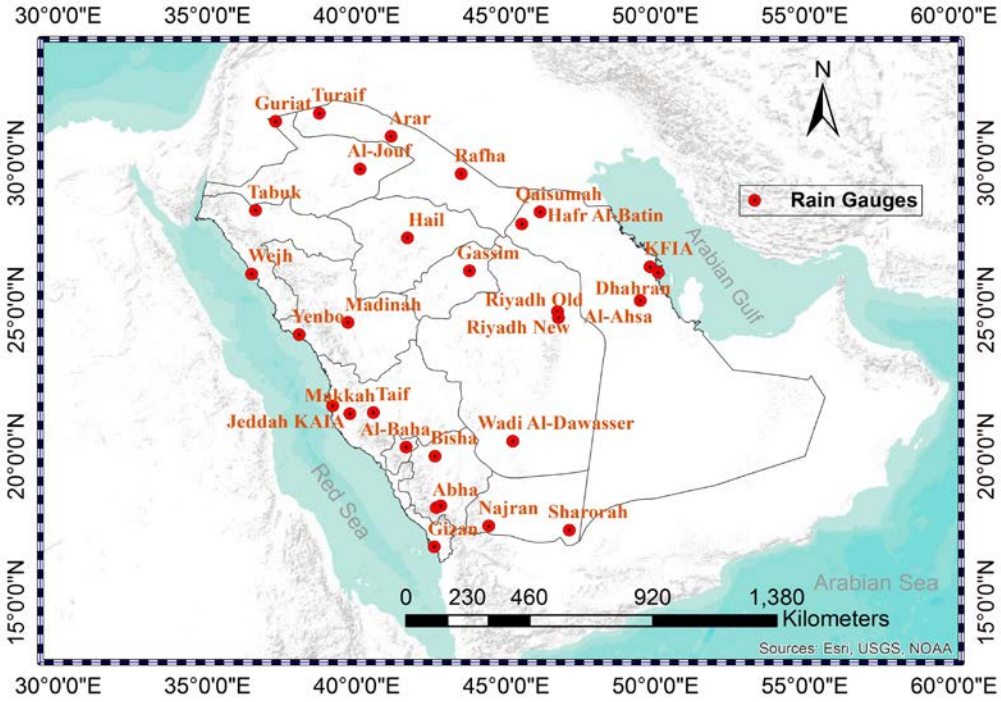

FIGURE 5. The spatial distribution of rain gauges over the provinces of Saudi Arabia.

The annual average precipitation recorded in the rain gages from 1985 to 2005 is shown in FIGURE 6 and FIGURE 7 shows temporal distribution of rainfall at the observation sites. Rain gauge "Abha" close to the Asir Mountain records annual average of about 300 mm, the highest amount of precipitation (FIGURE 6). As mentioned earlier, this region is subjected to monsoons from Indian Ocean, usually occurring between October and March and approximately 60 percent of the annual total falls during this period (FIGURE 7).

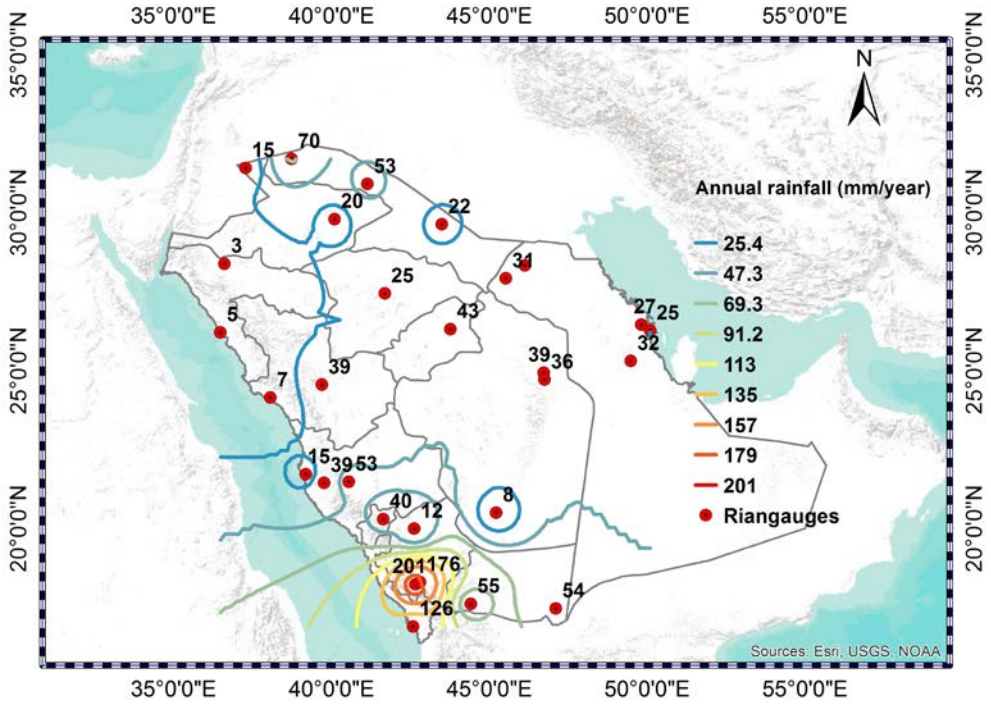

FIGURE 6. Average annual precipitation represented in isohyet contour lines for rain gauges over Saudi Arabia.

Generally, the highest amount of rainfall over kingdom occurs in the spring season and lowest amount in the summer. The lowest amount of rainfall occurs over the north and northwest areas. The south east, a deserted area, does not have any meteorological station and no information on rainfall is known.

2.2.1 Satellite Data

There are number of satellite-derived precipitation products were available at very high spatial (0.25° latitude×0.25° longitude grid size) and temporal (three hourly) resolution. For this study four satellite products were evaluated: TMPA product (Huffman et al. 2007) 3B42, which are produced by the TRMM project at the National Aeronautics and Space Administration; PERSIANN (Hsu et al. 1997) from the University of California, Irvine; CMORPH (Joyce et al. 2004), which is produced by NOAA/CPC; and GSMaP from Osaka Prefecture University in Japan (Okamoto et al. 2007). GSMaP

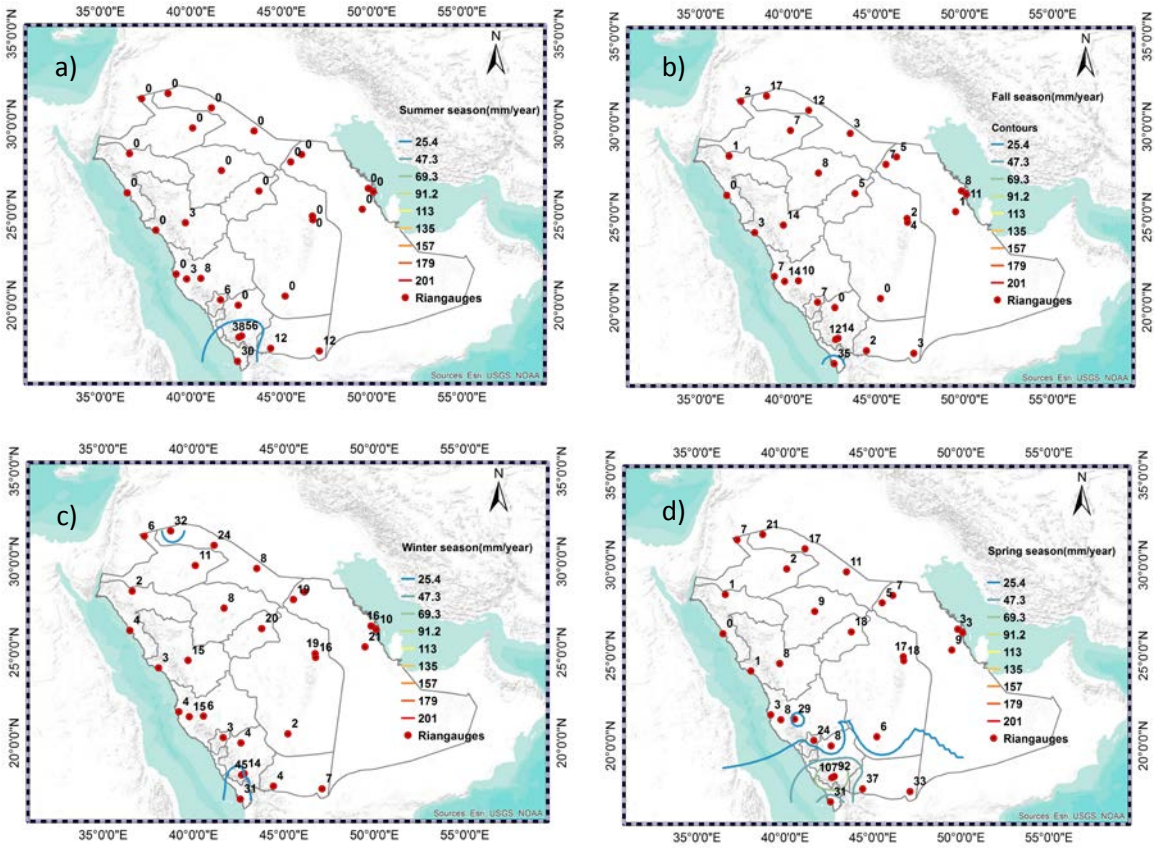

FIGURE 7. Average annual precipitation isohyetal contour lines over Saudi Arabia in (a) the summer, (b) the autumn, (c) the winter, and (d) spring season.

products, GSMaP moving vector with Kalman filter (GSMaP-MVK). A brief description of satellite products follows in this chapter, explaining why they were selected.

2.2.1.1 TRMM. The Tropical Rainfall Measuring Mission (TRMM) is a joint U.S.-Japan satellite mission to monitor tropical and subtropical rainfall. The primarily rainfall sensors on board the TRMM spacecraft are the Precipitation Radar (PR), the TRMM Microwave Imager (TMI), and the Visible and Infrared Scanner (VIRS). The TRMM standard products are classified into three levels: level one product is the calibrated and geolocated raw data. Level two products are derived geophysical parameters at the same resolution and location as those of the level one source data. Level 3 product, known as climate rainfall products, is the time-averaged parameters mapped onto a uniform space-time grid (Feidas et al. 2009). For this study, TRMM climate rainfall product 3B42 is used which is derived from TRMM Multi-Satellite Precipitation

Analysis (TMPA) algorithm. The algorithm combines infrared (IR) data from geostationary satellites, which have better sampling frequency but poorer quality, and passive microwave (PM) data, which has high quality but low sampling frequency, from different sources in four steps:

1. The different PM estimates are adjusted and combined,
2. IR precipitation estimates are created using the PM estimates for calibration,
3. PM and IR estimates are combined, and
4. The final product is rescaled to monthly totals. Monthly rainfall from the Climate Assessment and Monitoring System (CAMS) or Global Precipitation

Climatology Center (GPCC) rain gauge analysis are merged optimally to create 3B42, a post-real-time monthly gauge adjusted satellite product (Huffman et al. 2007).

The product produced from the third step of TMPA algorithm is 3B42RT that is near-real-time version and which are not bias corrected unlike the product produced in the fourth step. While 3B42RT is available with a lag time of a few hours after the IR and PM inputs are available, 3B42 product is available 2 days after the end of each month. The dataset is available at three-hourly temporal and 0.25^{o} spatial grid resolution between 50°N and 50°S and from the period of January 1998 to present. In some regions 3B42RT product has performed better than 3B42 (Dinku et al. 2009) but in general the later product is expected to have higher quality than the former product.

2.2.1.2 PERSIANN. The Precipitation Estimation from Remotely Sensed Information using Artificial Neural Networks (PERSIANN) algorithm uses a three-layer feed forward artificial neural network (ANN) technique to estimate rainfall rates from IR images (Hsu et al. 1997) of the global geosynchronous satellites provided by the Climate Prediction Center (CPC), NOAA (Janowiak et al., 2001), as the main source of information. ANN, an adaptive training technique, uses infrared brightness temperature (Tb) of the pixel, mean Tb of the 3 × 3 and 5 × 5 pixel windows around the pixels of interest, and standard deviations of Tbs in these windows. Initially the ANN was trained using radar data and the input was limited to IR data.

The recent version also uses daytime visible imagery (Hsu et al. 1999) and the TRMM microwave Imager rainfall estimates (2A12) to update the ANN parameters (Sorooshian et al. 2000). The rainfall data is available since 2000 at daily timescale and at 0.25-degree-by-0.25-degree spatial resolution and is used in this study. FIGURE 8

shows the rain estimation by PERSIANN algorithm over the Saudi Arabia region on Nov 25, 2009.

2.2.1.3 CMORPH. CMORPH (CPC MORPHing technique) rainfall product is the produced at NOAA's Climate Prediction Center (CPC). The product produces global precipitation analyses at very high spatial (grid size of 8 km at the equator) and temporal resolution (half hourly) by incorporating various passive microwave rain estimates derived from the following passive microwaves sensors:

(a) Special Sensor Microwave Imager (SSM/I) carried aboard the Defense Meteorological Satellite Program (DMSP) satellite 13, 14, and 15.

(b) Advanced Microwave Sounding Unit-B (AMSU-B) aboard NOAA's satellite 15, 16, 17, & 18.

(c) Advanced Microwave Scanning Radiometer (AMSR-E) and TRMM microwave Imager (TMI) aboard NASA's Aqua and TRMM satellites.

However, vast areas of the globe may have gaps because of insufficient global coverage by PM sensors at a 30-min time scale only. Therefore, the technique combines the PM rainfall estimates that have better accuracy with thermal IR observations, which has better sampling frequency where PM rain estimates are not available (Joyce et al. 2004). At a given location, the shape and intensity of the precipitation features in the intermediate half hour periods between microwave scans is generated by a time – weighting interpolation of features that have been propagated forward in time from the previous microwave observation and those that have been propagated backward in time from the following microwave scan (Joyce et al. 2004). The final product is a spatially and temporally complete PM rainfall estimate, which is independent of the thermal IR

rainfall estimates. The precipitation products are available (8 km at the equator) although the resolution of the individual satellite-derived estimates is coarser than that - more about 12 x 15 km or so. Method of interpolation is used to generate the finer resolution precipitation estimates. This data is available from 2002 to present. CMOPRH estimated precipitation over study region on Nov 25, 2009 is shown in FIGURE 8.

2.2.1.4 GSMaP MVK. The Global Satellite Mapping of Precipitation moving vector with Kalman filter (GSMaP-MVK) project was initiated to produce a high precision, high-resolution global precipitation map using satellite data and is sponsored by Core Research for Evolutional Science and Technology (CREST) of the Japan Science and Technology Agency (JST). Similar to the algorithm of CMORPH, the GSMap-MVK algorithm combines PM rainfall estimates from TRMM TMI, Aqua AMSR-E, DMSP SSM/I and Special Sensor Microwave Imager/Sounder (SSMIS), NOAA AMSU-A/-B and Microwave Humidity Sounder (MHS), MetOp AMSU-A and MHS of European Organization for the Exploitation of Meteorological Satellites (EUMETSAT) with IR rain data from Geostationary Operational Environmental Satellite 8 and 10, Meteosat 5 and 7, and Geostationary Meteorological Satellite (GMS). But the difference between CMORPH and GSMap-MVK is that CMORPH uses the thermal IR observations only to extract information about the time evolution of the PM rain rates, while not GSMaP-MVK not only uses IR information for time evolution but also uses the IR rainfall estimates at times the PM estimates are not present along with the propagated PM estimates within a Kalman filter framework (Okamoto et al. 2007). Data is available from 2003 to 2009 at 0.1^{o} spatial and hourly temporal resolution.

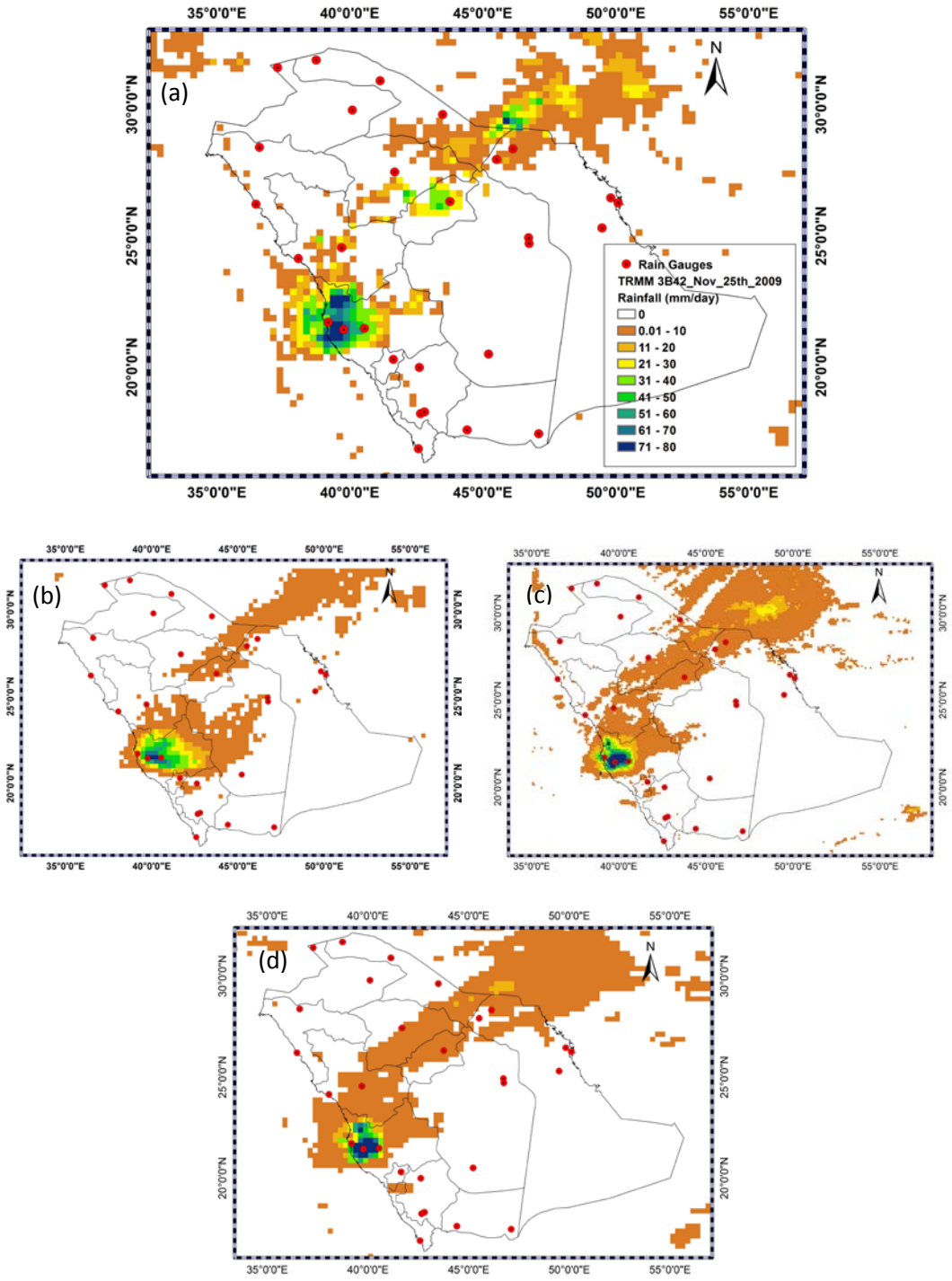

FIGURE 8. Precipitation estimated by TRMM 3b42 (a), PERSIANN (b), GSMaP_MVK v5.2221 (c) satellite, and CMORPH (d) satellite over the study region on Nov 10, 2009.

FIGURE 8 shows the precipitation estimated by the four satellites over the study region on November 25, 2009 when a major flood event occurred on the western side of the country. On this day, TRMM 3B42 and PERSIANN show more than 40 mm rainfall on the southwest of the study area. Both CMORPH and GSMaP_MVK have identified rain over the region but with 49 mm.

FIGURE 9 shows the peak rainfall over the area on November 25, 2003. On this day, TRMM 3b42 and PERSIANN showed an overestimation with 40 mm and 81 mm while the rain gauge detected 13 mm over Jeddah rain gauge. Even CMORPH and GSMaP_MVK depicted 89 mm over the area, which represent a huge overestimation with regard to the rain gauge detection at that day.

2.3 Statistical Methods

Analyses of daily, 10-daily, and monthly estimate of all above-mentioned precipitation remote sensing products. The analysis methods used to validated these products are Probability of Detection (POD), False Alarm Ratio (FAR), Frequency of bias (FBS), Probability of False Detection (POFD), Bias, Mean Error (ME), Mean Absolute Error (MAE), Efficiency (Eff), Correlation Coefficient (CC), Root Mean Square Error (RMSE), Hanssen-Kuipers Skill Score (KSS), Threat Score (TS) or Critical Success Index (CSI), and Heidke Skill Score (HSS), using all of those statistical methods of validation to assess the accuracy of each product against the rain gauge ground observations, and compare their percent of agreement against each other and the precipitation ground observing network. According to the Presidency of Metrological and Environment (PME), the Kingdom of Saudi Arabia rain gauges network includes 29 ground gauges distributed vastly across the region, which the study is focusing on form 2003 to 2011 period. The location lacks sufficient precipitation observing networks required for water resources controlling, atmospheric analyses, and natural dangers mitigation. This is true in

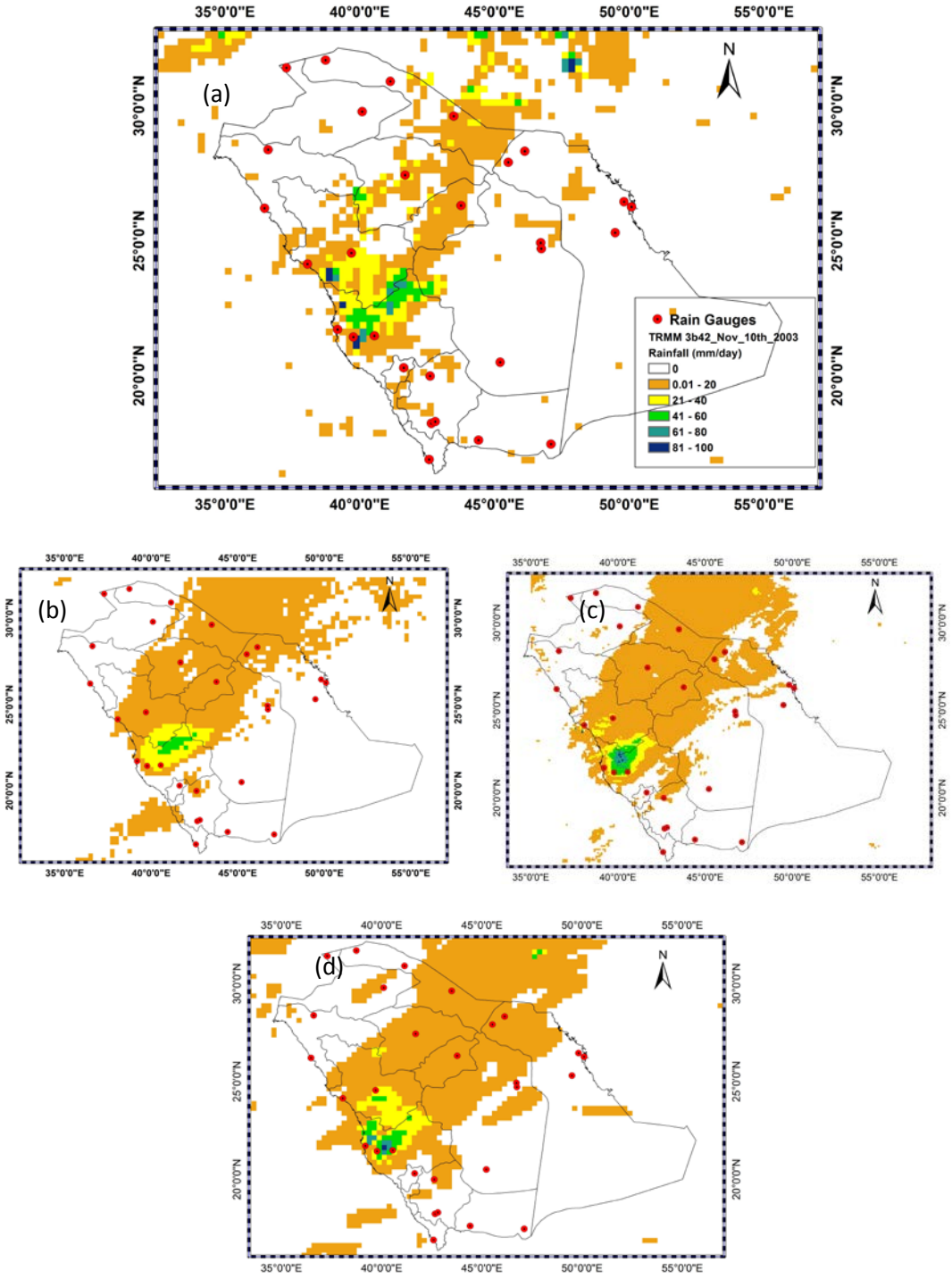

FIGURE 9. Precipitation estimated by TRMM 3b42 (a), PERSIANN (b), GSMaP_MVK v5.2221 (c), and CMORPH (d) satellites over the study region on Nov 10, 2003.

TABLE 4. The Contingency Table Shows the Binary and Corresponding Observations

Event forecast/predicted by satellite	Event Observed at Rain Gauge	
	YES	NO
YES	A	B
NO	C	D

Note: The rainfall threshold is >= 1.0 mm.

particular with complex terrain regions where urban areas and infrastructures are sparse as in our study area. The region needs the categorical statistics to evaluate the binary hits/ misses estimates of type of statement an event will or will not occur.

2.3.1 Probability of Detection (POD)

The measure that examines the event by measuring the proportion of observed events that actually occurred and detected by the rain gauge is Probability of Detection:

$$POD = \frac{A}{A + C} \quad (1)$$

Range of POD is zero to one, as one is the perfect score. It is also known as the Hit Rate. The POD gives the Hit rate, which gives the relative number of real rainfall events. POD is sensitive to hits but takes no account for false alarms. It is our intention to get the maximum number of hits and minimize the number of false alarms and misses to get adequate estimates for the tested satellite product.

2.3.2 Frequency Bias (FBS): The Amount of Estimation Errors

The frequency of binary precipitation events compares the frequency of precipitation estimates to the frequency of the actual occurrence and is represents by ratio.

FBS ranges between zero to infinity, an unbiased score= 1. With FBS >1 (<1), the precipitation estimate system exhibits overcasting (under-forecasting) of events.

$$FBS = \frac{A+B}{A+C} \tag{2}$$

2.3.3 False Alarm Ratio (FAR)

This method detects the false alarm events from the data sets of the population investigated:

$$FAR = \frac{B}{A+B} \tag{3}$$

Range of FAR is zero to one, as zero is a perfect score. Contrary to POD, FAR is sensitive to false alarms but takes no account of misses. FAR has a negative orientation. Also, FAR is very sensitive to climatological frequency of the event.

2.3.4 Probability of False Detection (POFD)

It is the opposite of False Alarm Ration purpose

$$POFD = \frac{B}{B+D} \tag{4}$$

The result magnitude of POFD is again one to zero with a perfect score = 0. POFD is generally associated with the evaluation of probabilistic of estimate the evaluation of probabilistic of estimate by combining it with POD.

2.3.5 Bias

The bias of gauge vs. satellite product verified compares the frequency of estimated to the frequency of the actual occurrence and represented by the ratio:

$$Bias = \frac{\Sigma S}{\Sigma G} \quad (5$$

Range of bias is zero to infinity, an unbiased score= 1. If Bias >1 the estimated system exhibits overestimation and if Bias <1 then it exhibits an underestimation.

2.3.6 Mean Error (ME)

This step is to compute the simple average difference between the estimated precipitation amount and the observation from the rain gauge, the Mean Error:

$$ME = \frac{1}{N}\sum(S - G) \quad (6)$$

The mean error is easiest and most familiar scores, it can provide useful information on the local behavior of a given weather parameter such as precipitation. The ME ranges from infinity and minus infinity, and the perfect score is = 0. However, it is possible to reach a perfect score for dataset with large errors, if there was a negative magnitude, which place errors. The ME is not an accuracy measure, as it does not give information of the amount of estimation errors.

2.3.7 Mean Absolute Error (MAE)

It is a simple test to compensate for the potential positive and negative errors of the ME, which is represented in this equation:

$$MAE = \frac{1}{N}\sum\frac{|(S-G)|}{G} \quad (7)$$

The MAE range is from zero to infinity and, as with ME, a perfect score= 0. The MAE measures the average magnitude of estimated errors in a given dataset and therefore is a scale of estimated accuracy.

2.3.8 Efficiency

Evaluate the performance of the satellite products in estimating the amount of satellite the rainfall.

$$\text{Eff} = 1 - \frac{\sum(S-G)^2}{\sum(G-\bar{G})^2} \quad (8)$$

Efficiencies can range from (−∞ to 1). An efficiency of 1 (Eff = 1) corresponds to a perfect match of modeled discharge to the observed data. An efficiency of 0 (Eff = 0) indicates that the model predictions are as accurate as the mean of the observed data, whereas an efficiency less than zero (Eff < 0) occurs when the observed mean is a better predictor than the model or, in other words, when the residual variance (described by the numerator in the expression above), is larger than the data variance (described by the denominator). Essentially, the closer the model efficiency is to 1, the more accurate the model (Nash and Sutcliffe 1970).

2.3.9 Correlation Coefficient (CC)

Person's Correlation Coefficient measures of the strength and direction of the linear relationship between two variables that is defined in terms of the (sample)

covariance of the variables divided by their (sample) standard deviations. The value of Pearson's correlation coefficient, unlike all other estimates for continuous dependent variables, is influenced by the distribution of the independent variable in the sample.

$$CC = \frac{\sum_{i=1}^{N}(Si-\bar{S})\,(Gi-\bar{G})}{\sqrt{\sum_{i=1}^{N}(Si-\bar{S})^2 \sum_{i=1}^{N}(Gi-\bar{G})^2}} \tag{9}$$

The correlation coefficient ranges from −1 to 1. A value of 1 implies that a linear equation describes the relationship between rain gauge data and satellite data perfectly, with all data points lying on a line for which satellite data increases as rain gauge increases. A value of −1 implies that all data points lie on a line for which satellite data decreases as rain gauge increases. A value of 0 implies that there is no linear correlation between the variables (Buda and Jarynowski 2010).

2.3.10 Root Mean Square Error (RMSE)

Root mean square is common accuracy measure. It is a statistical measure of the magnitude of a varying quantity. It is especially useful when it used to assess the accuracy of the satellite data versus raingear data.

$$\mathbf{RMSE} = \frac{1}{N}\sum (S-G)^2 \tag{10}$$

Root mean square error has the same unit as the estimate satellite precipitation parameter. The RMSE ranges from zero to infinity with a perfect score = 0. The RMSE is the squared difference between the estimate satellite precipitation and observation. Due to the second power, RMSE is much more sensitive to large estimates from satellite error than MAE is. This may be harmful in the presence of potential outliners in the datasets

and, consequently, at least with small or limited datasets the use of the MAE is preferred (Nurmi 2003).

2.3.11 Hanssen-Kuipers Skill Score (KSS)

Is defined as it simplest form. It is also known as True Skill Statistics (TSS)

$$KSS = \frac{AD\text{-}BC}{[(A+C)(B+D)]} \quad (11)$$

KSS ranges from minus one to one, with a perfect score = 1, no skill estimate= 0. Ideally, KSS measures the ability of the estimate product to separate POD values from cases of POFD.

2.3.12 Threat Score (TS) or Critical Success Index (CSI)

This test method is widely performance evaluator of seldom events.

$$TS = \frac{A}{A+B+C} \quad (12)$$

Threat score ranges between zeros to one with a perfect score. No skill estimate =0. Threat score is sensitive to hits, take into consideration both false alarms, misses, and can be seen as a measure for the event of being estimated after removing correct estimate from consideration.

2.3.13 Heidke Skill Score (HSS)

$$HSS = \frac{2(AD\text{-}BC)}{(A+C)(C+D)+(A+B)(B+D)} \quad (13$$

It is reference accuracy measure proportion correct, adjusted to neglect estimates, which would be correct to random chance. HSS ranges from minus infinity to one with a perfect score = 1, no skill estimate would be equal to zero.

Following statistics were used to evaluate hydrologic model.

2.3.14 Nash-Sutcliffe Efficiency (NS)

The Nash–Sutcliffe model efficiency coefficient is used to assess the predictive power of hydrologic model. It is defined as:

$$NS = 1 - \frac{\sum_{t=1}^{n} (Q_o^t - Q_m^t)^2}{\sum_{t=1}^{n} (Q_o^t - \overline{Q}_o)^2} \quad (14)$$

where, Q_o is observed discharge, and Q_m is the discharge predicted by the model. Q_o^t is observed discharge at time t. Nash–Sutcliffe efficiencies can range from $-\infty$ to 1. An efficiency of 1 (NS = 1) corresponds to a perfect match of modeled discharge to the observed data. An efficiency of 0 (NS= 0) indicates that the model predictions are as accurate as the mean of the observed data, whereas an efficiency less than zero (NS < 0) occurs when the observed mean is a better predictor than the model. Essentially, the closer the model efficiency is to 1, the more accurate the model is. If NS>= 0.7, the model has a good performance.

2.3.15 Coefficient of Determination (R^2)

Degree of collinearity between simulated and observed data can be measured using coefficient of determination (R^2). The coefficient can ranges from 0 to 1 with higher values indicating less error variance, and typically values greater than 0.5 are considered acceptable. If R = 0, no linear relationship exists. The statistic is oversensitive to high extreme values.

CHAPTER 3

VALIDATION AND RESULTS

3.1 Validation Results

To measure the accuracy of satellite rainfall estimates from TRMM 3B42, PERSIANN, and CMORPH rainfall data were collected for the study period of January 2003 to December 2011 and precipitation data from GSMaP_MVK (V5.222) were collected from the period of January 2003 to November 2010. The satellite precipitation data is evaluated at daily, 10-daily, and monthly time scale using different conventional statistical methods that are described in Chapter 2. Rainfall estimates from each satellite pixel that overlapped at least one rain gauge location is considered for validation study.

3.2 Validation at Daily Timescale

TABLE 5 shows the results of daily validation for CMORPH, PERSIANN, TRMM 3B42 V. 7, and GSMaP_MVK V. 5.2221 rainfall retrieved estimates results obtained by comparing the daily rainfall data from all 29 rain gauge stations and overlapping satellite pixels. The results show CMORPH and GSMap have higher probability of detection (POD) and PERSIANN has the least. False alarm ratio (FAR) is also high for PERSIANN rainfall estimates while other satellites have similar FAR value. The detection capability of different satellite products is also measured using correlation coefficient (CC). None of the products has higher correlation coefficient value but PERSIANN shows least correlation with gauge observation. Therefore, in terms of

rainfall detection across the country TRMM, GSMap, CMORPH show statistical similarity, GSMap, and CMORPH stand out with better performance.

Statistics like mean error (ME), mean absolute error (MAE), bias, root mean square error (RMSE), and frequency bias (FBS) are used to evaluate the accuracy of satellite rainfall estimates. TRMM also has the least and PERSIANN has the highest MAE and RMSE value. The difference in MAE and RMSE suggests that there is not a significant variance in data for any one the satellite products. However, all the products shows overestimation (bias >1) and frequency (FBS>1) of rainfall. GSMap, CMORPH have the higher and TRMM has the least ME values all the products have positive ME value which indicate forecast, on average is high. FIGURE 10 helps to see the distribution of the precipitation bias at different rain gauge locations. TRMM, which has the least average bias among the four products, show some underestimation in the southern part and overestimation at rest of the rain gauge locations. The bias at southwestern region is more than other locations. CMORPH, PERSIANN, GSMap also show higher bias at the southwestern gauges with significant increase in bias at the observation station at the southwest corner. Similar results can be seen from the wider spread of the scatter plot in FIGURE 11. Forecast skill of the satellite products were assessed using Threat score (TS), Heidke skill score (HSS), and Hanssen-Kuiper skill score (KSS). Values of TS for all the satellites are less than 0.5. KSS value is positive for all the products indicating that POD is more than FAR. This is also reflected with the low value of probability of false detection (POFD). Values of HSS are similar to correlation coefficient and it indicates the proportion of the rainfall detection accuracy by random chance.

TABLE 5. Validation Statistics Comparing the Performance of Daily Satellite Rainfall Estimate

	TRMM 3b42	PERSIANN	GSMaP MVK	CMORPH
FBS	1.26	1.60	1.72	1.61
POD	0.39	0.24	0.53	0.52
POFD	0.02	0.04	0.03	0.03
FAR	0.62	0.84	0.67	0.66
Bias	1.14	1.48	1.63	1.53
CC	0.44	0.11	0.45	0.44
ME	0.26	0.30	0.65	0.62
MAE	1.50	2.20	1.84	1.72
RMSE	2.092	2.658	2.288	2.968
TS	0.22	0.11	0.26	0.26
KSS	0.36	0.20	0.50	0.49
HSS	0.34	0.17	0.38	0.39

Among the four satellite products, CMORPH and GSMap have highest probability of detection (POD) shown in FIGURE 11 but TRMM 3B42 has least bias, MAE, RMSE, and ME. Rainfall product from PERSIANN has larger overestimation, False Alarm Ratio depicted in FIGURE 12 and least correlation coefficient in FIGURE 13, and probability of detection than the others.

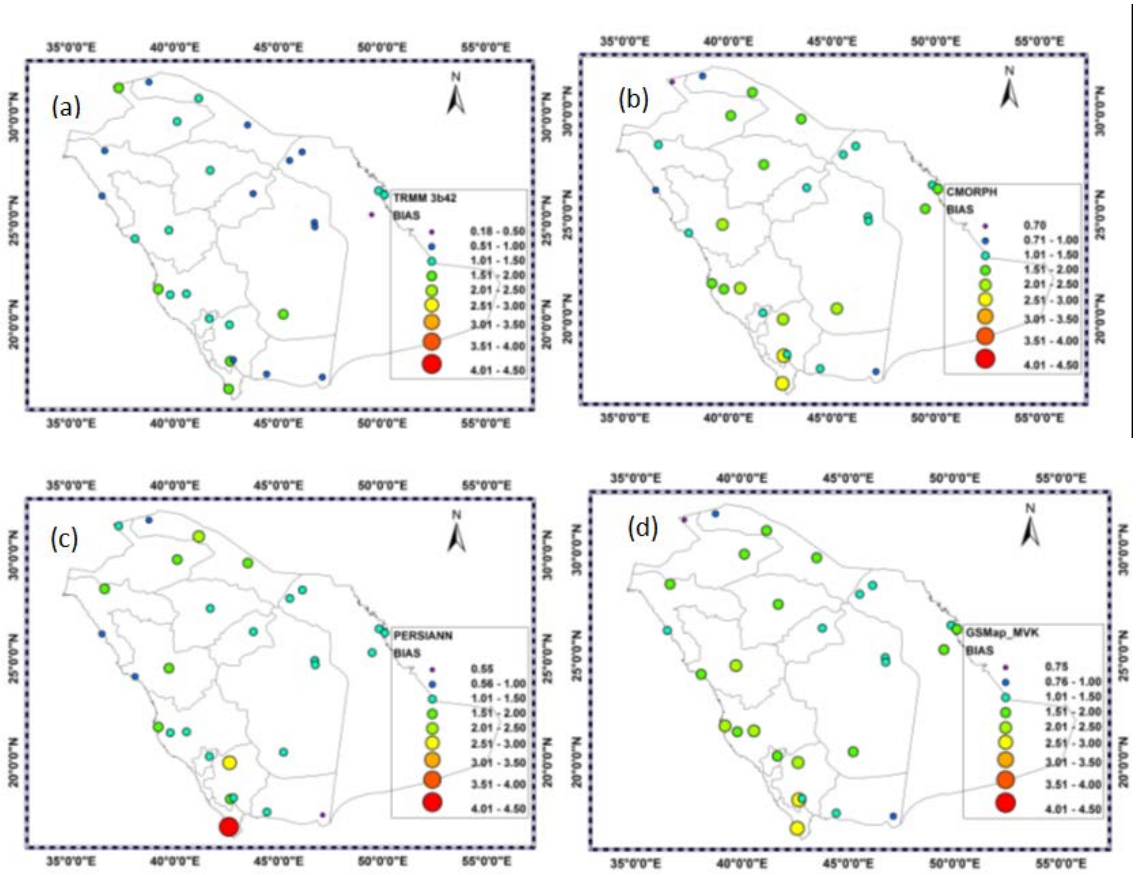

FIGURE 10. BIAS daily spatial distribution of satellite products (a) TRMM 3B42 (b) CMORPH (c) PERSIANN and (d) GSMaP_MVK at daily timescale.

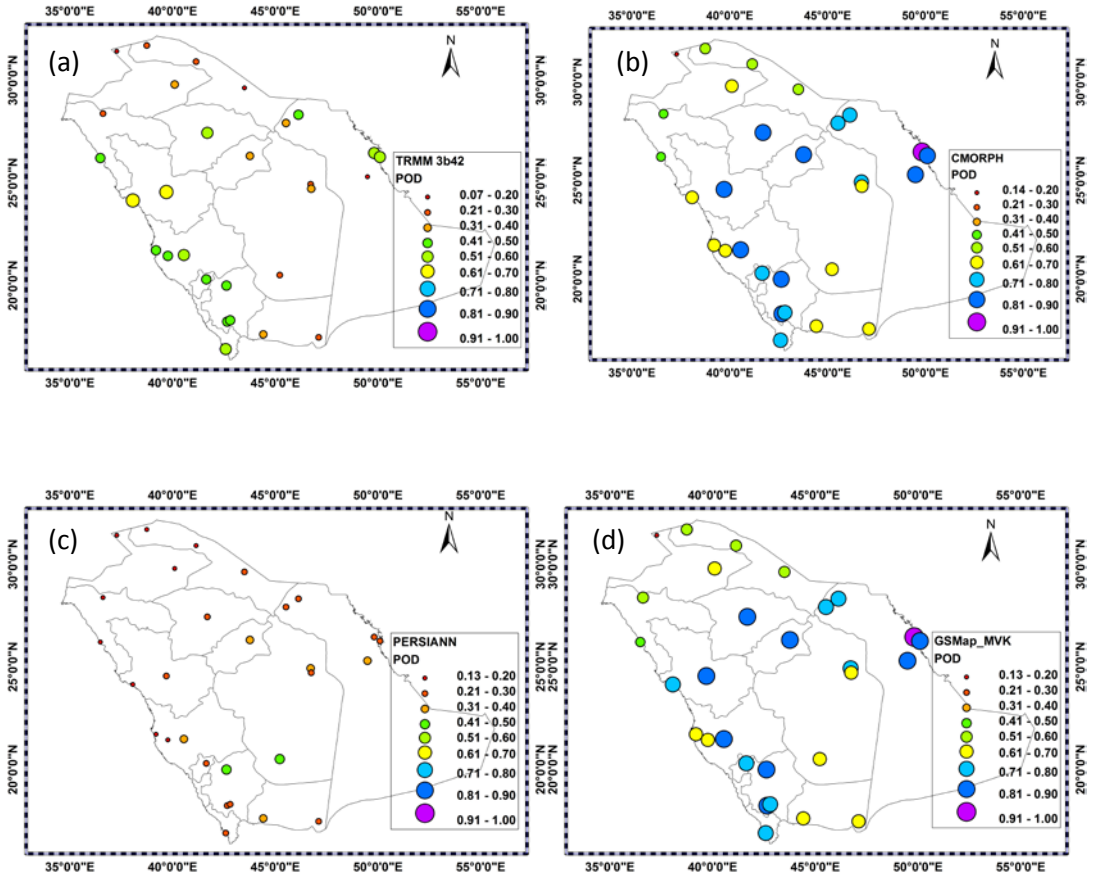

FIGURE 11. POD daily spatial distribution of satellite products (a) TRMM 3B42 (b) CMORPH (c) PERSIANN and (d) GSMaP_MVK at daily timescale.

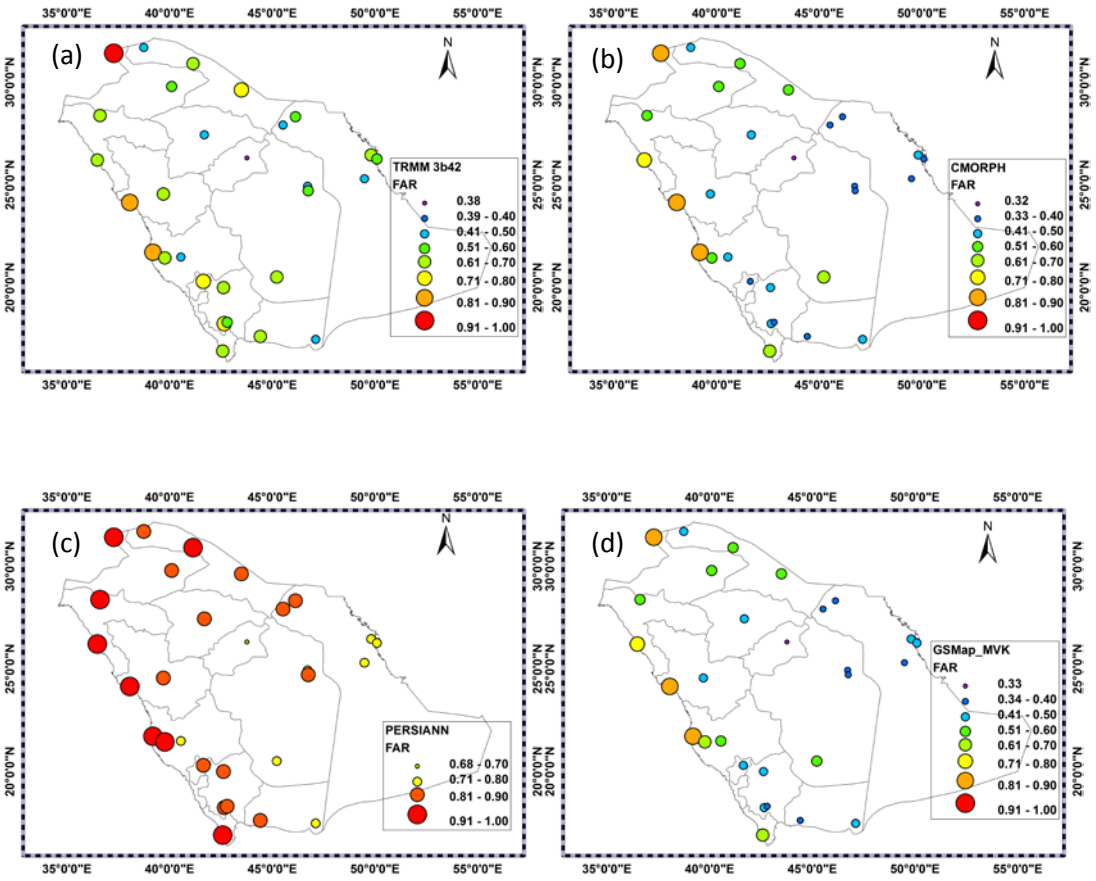

FIGURE 12. FAR of daily satellite products (a) TRMM 3B42 (b) CMORPH (c) PERSIANN and (d) GSMaP_MVK at daily timescale.

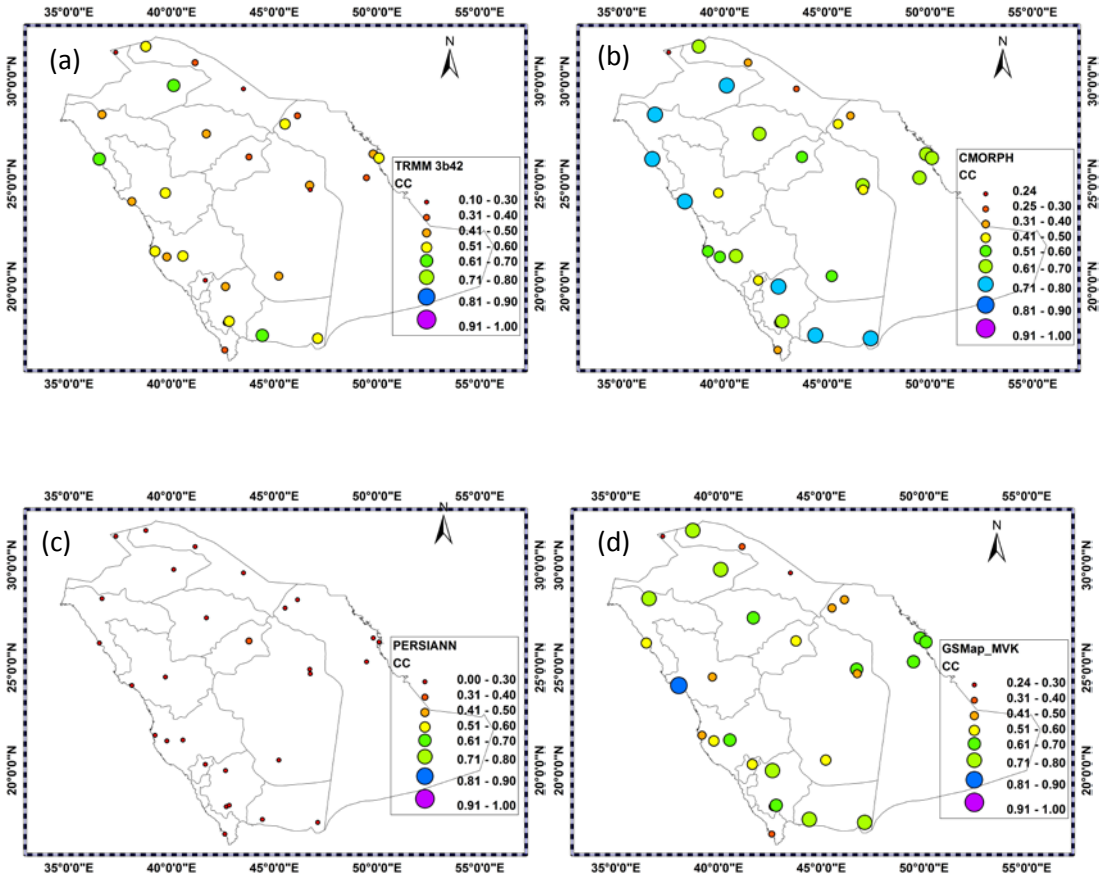

FIGURE 13. Correlation coefficient (CC) of daily satellite products (a) TRMM 3B42 (b) CMORPH (c) PERSIANN and (d) GSMaP_MVK at daily timescale.

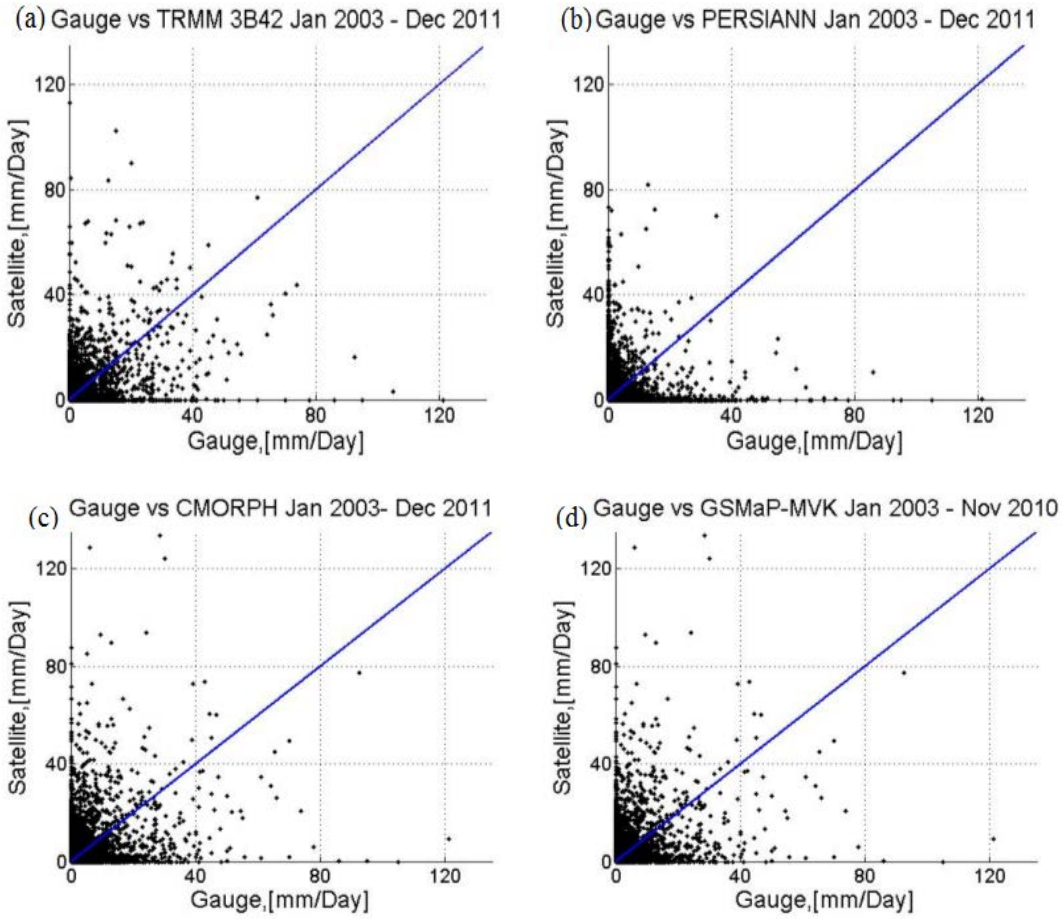

FIGURE 14. Comparison of the performance of detecting rainfall estimates over Saudi Arabia at daily, time scale and 0.25° long/let special resolution.

3.3 Validation at 10-Daily Timescale

The satellite products are also evaluated at 10-daily time scale. The rainfall estimates from each pixel of 0.25° (0.1° in GSMaP_MVK) resolution that include at least one rain gauge location is accumulated over the 10-day period. For comparison of temporal accumulation, the resolution of the grid is kept same. The validation at 10-daily resolution frequency bias, POD, POFD, FAR, TS, KSS, and HSS are not evaluated because at this temporal scale detection capability is not an issue. Skill of rainfall

estimates is assessed using bias, correlation coefficient, mean error, mean absolute error. An additional statistics, efficiency is used to evaluate the accuracy of rainfall estimates with respect to the average rain gauge measurements for all time periods (Dinku et al. 2010). After applying all the statistical formulas, the validation results of 10-Daily rainfall accumulation are presented on TABLE 6. Results show that there is an increase in the correlation coefficient, also a decrease in MAE, with no change in the bias value. TRMM has highest correlation coefficient and least MAE. TRMM also shows least bias over the daily accumulation. Compared to daily statistics, all the products have increased mean error and RMSE while TRMM has the least mean error and RMSE. The Eff statistics show that the all the products have reasonable skill in rainfall estimation. TRMM show highest Eff skill compared to other products.

TABLE 6. Validation Statistics Comparing the Performance of 10-Daily Satellite Rainfall Estimate

	TRMM 3b42	PERSIANN	GSMaP MVK	CMORPH
Bias	1.14	1.47	1.61	1.52
EFF	0.81	0.46	0.59	0.65
CC	0.63	0.37	0.58	0.57
ME	0.51	0.95	0.73	0.73
MAE	0.26	0.46	0.39	0.38
RMSE	6.364	9.7573	8.424	8.379

Validation results of rainfall estimates at 10-daily temporal accumulation show TRMM exhibits best performance in all the statistics. Scatter plot of 10-daily accumulated rainfall estimates and gauge measurement shown in FIGURE 15 presents similar result. At this temporal scale, performances of all the products have improved and TRMM shows lesser scatter of the data points.

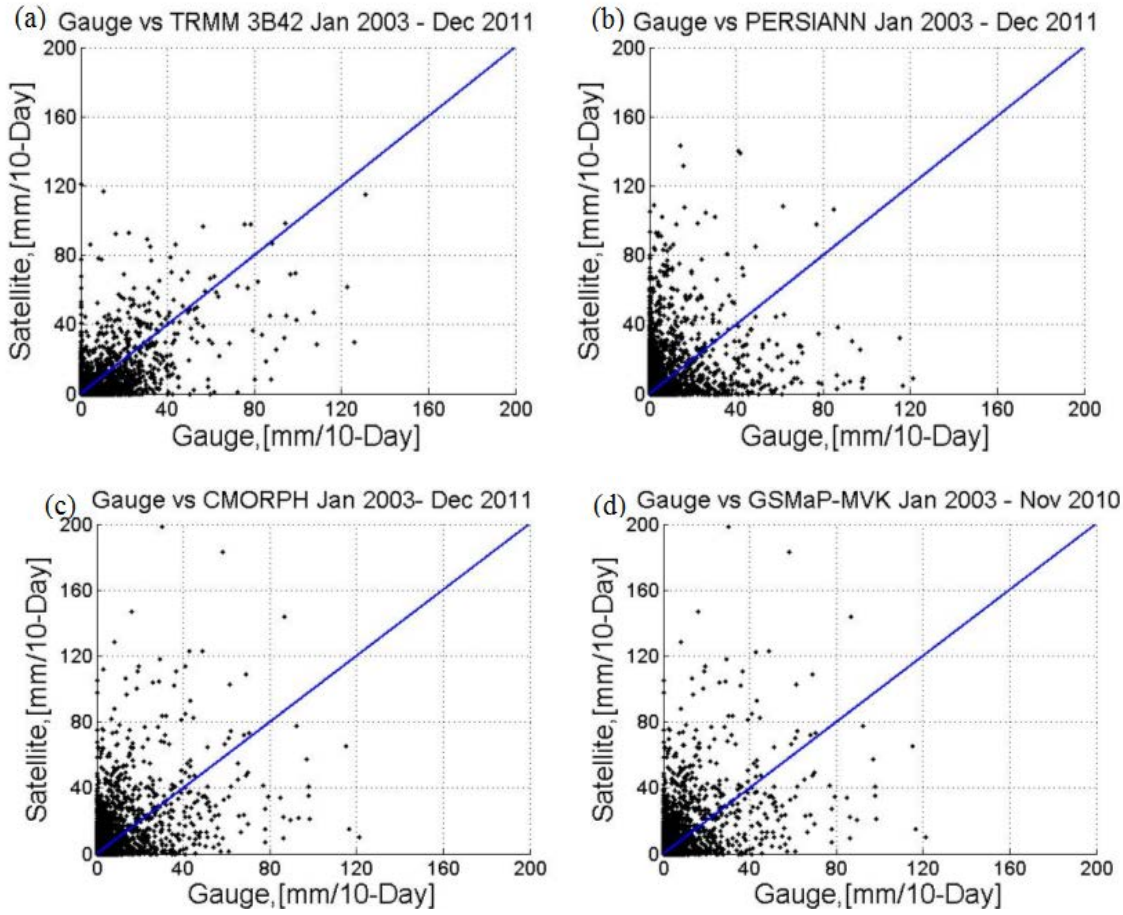

FIGURE 15. Comparison of the performance of detecting rainfall estimates over Saudi Arabia at 10-daily, time scale, and 0.25° long/lat special resolution.

3.4 Validation at Monthly Time Scale

Different validation statistics were also assessed at monthly scale. Bias, efficiency, means absolute error, and correlation coefficient at different months is compared in FIGURE 16. TRMM shows overall very little bias. However, in during the summer month TRMM show increased bias. Similarly, PERISANN, CMORPH, and GSMap overestimate rainfall in the summer as well as in autumn and underestimates in the winter months. Among the four products, PERSIANN shows highest bias in summer and autumn. Results of efficiency also show that PERSIANN has no forecast skill in summer and autumn months. TRMM has overall better forecast efficiency.

The four products show varying correlation coefficients (CC) throughout the year. All the products show increased correlation coefficients in the months of February and August. TRMM shows least correlation coefficient in March and PERSIANN has least CC value in March. TRMM, PERSIANN, and CMORPH have positive mean absolute error (MAE) throughout the year while PERSIANN show highest variance in MAE value. Rain estimates from GSMap has negative MAE values in winter and positive MAE rest of the year. Scatter plot of monthly-accumulated rainfall from gauge and satellite observation is shown in FIGURE 17. At monthly scale, all the four satellite products presents greater agreement with gauge observation but TRMM 3b42 has more symmetrical scatter.

3.5 Discussion

The satellite rainfall estimates exhibit-varying agreement with gauge observation at different temporal resolution. At daily time scale, all of the four products show similar rainfall estimation capability although CMORPH and GSMap have highest detection

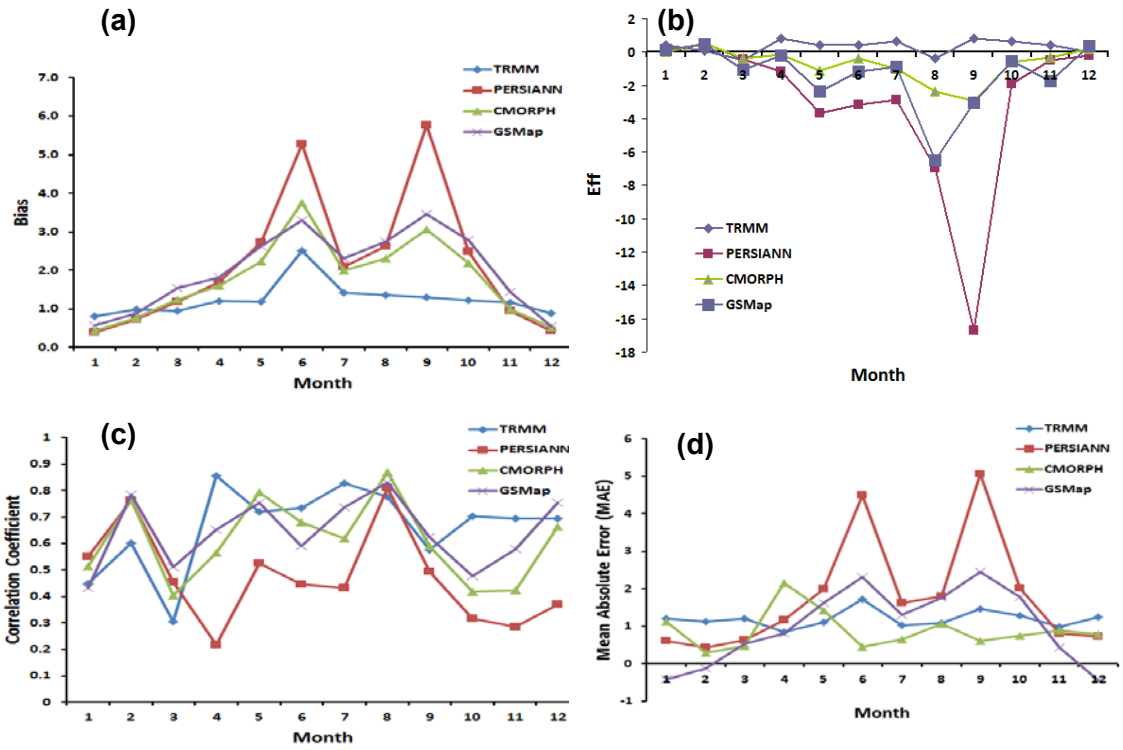

FIGURE 16. Monthly validation statistics of (a) Bias, (b) Efficiency, (c) Correlation Coefficient, and (d) Mean Absolute Error of the four satellite products over the region.

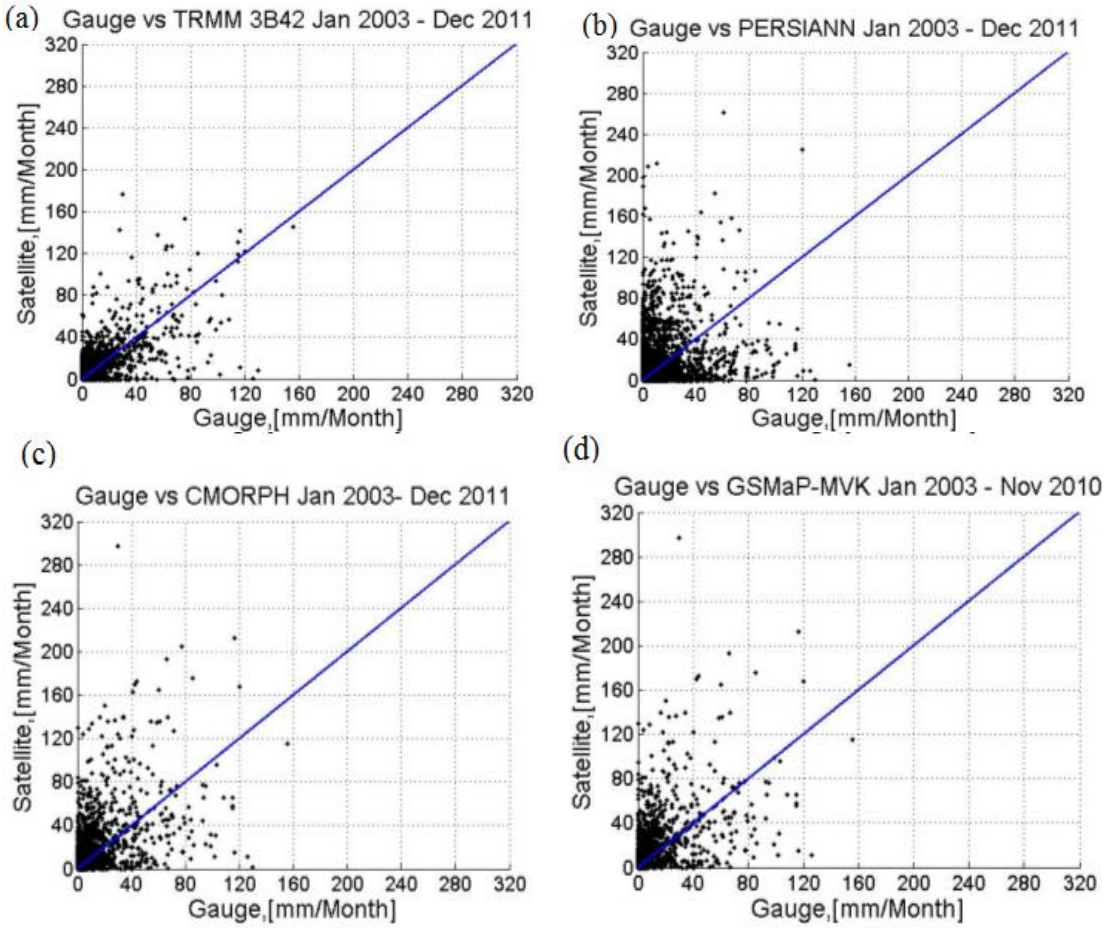

FIGURE 17. Scatter plot rainfall estimates over Saudi Arabia at monthly time scale and 0.25° long/ lat special resolution of four different satellite products.

probability and TRMM has the least false alarm ratio. Statistics calculated to measure accuracy of estimates show TRMM is a better rainfall estimator with least ME, MAE, RMSE values. Although all the products overestimate rainfall, TRMM has the least bias. The performance of satellite rainfall estimation increases at 10-daily time scale and TRMM rainfall estimates show better agreement with gauge observation. Comparison with monthly rainfall accumulation show seasonal variation of validation matrices.

During summer, when the region has less rain, all the satellite products show rainfall. Thus bias and MAE increases, efficiency and correlation coefficient decreases.

Among the products studied here, TRMM stand out as a better rainfall estimator at daily, 10-daily, and monthly time scale. Despite that, all the products have good agreement in with wintertime rainfall. During this period, country receives most of the rainfall and the recent flood events happened later in November. Therefore, all the four products are selected to study the hydrologic response in a western watershed in the city of Jeddah where records show devastating effect of flash flood events.

CHAPTER 4

HYDROLOGIC MODELING

4.1 Background

Runoff modeling has evolved appreciably since its innovation in the early years of the twentieth century. These phases relate to both common concerns and computational capabilities that were available during each of the periods. With the recent intensive rainfall that is falling out on the studied basin located in Saudi Arabia, Jeddah depicted by the rain gauges within the afflicted basin. These rain gauges are not detecting with high accuracy the rainfall behavior in the region. Therefore, an alternative to detecting precipitation was suggested to assessment as another method of precipitation detection. TRMM 3b42, PERSIANN, CMORPH, and GSMap_MVK v.5.2221 have been simulated using SWAT Model to estimate the surface runoff resulting from rainstorms for the period of 8-year (2003 to 2010). This model helps with ungauged basins such as the study area and can spatially interpolated with high accuracy precipitation from neighboring rain gauges as well as other functions. It leads to a requirement of long-term continuous simulation. The development and efficient utilization of the renewable sources of water in wadis is the optimal solution for addressing water shortage problems. The efficiency of harnessing water from wadis will depend on the understanding and knowledge of the qualitative and quantitative hydrology and water resources. In order to plan, design, and operate water resources projects, it is needed to model and measure

basic water variables such as rainfall, runoff, infiltration, floods, evaporation, and other hydrological attributes. The potential of water resources in the study watershed is narrow but due to the wadi effect, this makes the region prone to flash floods especially in the winter season (November to January). The watershed environment is barren in the upstream region, and urban in the downstream with limited vegetation representation. The goal in this study is to assess the runoff carried by the TRMM and PERSIANN remotely sensed precipitation products simulated by SWAT Model (Soil Water Assessment Tool).In this study, a simulation of surface runoff is implemented encompassing the entire watershed represented in FIGURE 18 on a daily basis as well as monthly basis to understand the behavior of the drainage area basin to urbanization. The results of simulation, surface runoff, and sediment yield are proposed as a tool to assess the flood effects within the area. Nevertheless, the results of simulation will not be calibrated due to unviability of stream gauges in the area of the watershed.

4.2 Objectives

The main objective of this chapter is to implement a physical-based runoff hydraulic model (SWAT) in small watershed in Saudi Arabia, Jeddah city.

To critically review the satellite precipitation products (TRMM, and PERSIANN).

To setup, SWAT to simulate wadi stream flow in upper bound of Jeddah watershed.

To apply SWAT model to assess 8-years period of runoff in the study watershed.

4.3 Study Area

4.3.1 Topography

The watershed in the study is located in Jeddah City (Makkah Province) centered in 39°19'55.8"E 21°31'16.7"N shown in FIGURE 18. It encompasses flood plain of a group of wadies to eastern side of the city. The high mountains (Tihamah) lie right to the basin with 711 m summit within the studied area. This watershed is categorized as urbanized area and semi-arid area. In 2009, the city was exposed to a devastating flood form one of the eastern wadi, which is referred to as Wadi Qows. Recently, this area has been affiliated with flash floods due to intense rainfall, accumulated sediments from the wadi, and lack of urban drainage system that can withhold huge amount of rainfall. The area of the basin is 124.095 km², longest path of 49 km², the average elevation is 182 m, mean slope 19.3% raise, and comprises of 13 sub-basins. From the Digital Elevation Model for Jeddah City, this is retrieved from USGS with 30 arc second resolution. Stream system was delineated associating DEM data.

4.3.2 Soil Characteristics and Classification

Soil dataset is taken form the FAO (Food and Agriculture Organization – United Nations) names and the corresponding Saudi Arabia soil nomenclatures in details in TABLE 7 and TABLE 8. The properties of each kind of soil are investigated and documented obviously in this study. The Soil Map from FAO of the World was published between 1974 and 1978. In general, the soil characteristics indicate that belongs to Sandy Clay Loam texture soil group of semi-arid and arid throughout the watershed. Soil moisture loss is greatly aggravated under the prevailing conditions of

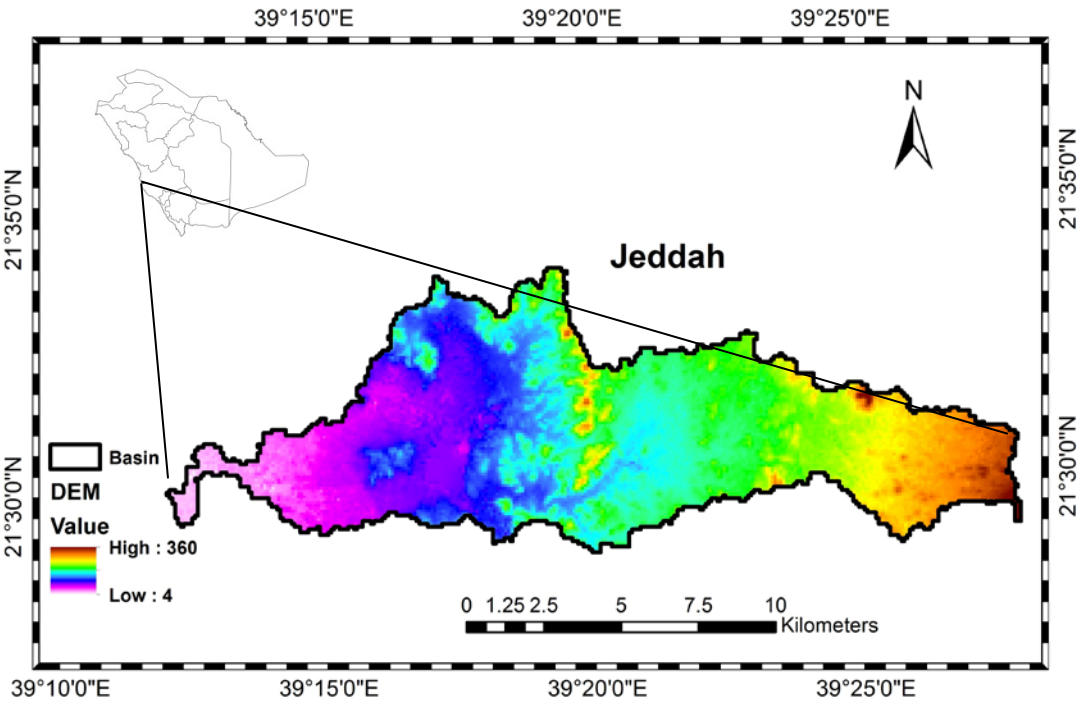

FIGURE 18. Jeddah city watershed located in Makkah Province.

high temperature, low humidity, intense radiation, and strong dry surface wind, with evaporation from surface soil tending to be high.

TABLE 7. Soil Properties as Retrieved from FAO Database

No.	FAO Name	Saudi Arabia Soil Taxonomy Acronym	Soil Hydrologic Group
1	Lithosols	I	B
2	Haplic Yermosols	YH	C

TABLE 8. Contents of Soil as Retrieved from FAO Database

Soil Unit Symbol	I	YH	Soil Unit Symbol	I	YH	Soil Unit Symbol	I	YH
sand % topsoil	58.9	50.4	OC % topsoil	0.97	0.3	CEC clay topsoil	55	60
sand % subsoil	56	40.8	OC % subsoil	0.4	0.2	CEC Clay subsoil	28	50
silt % topsoil	16.2	29	N % topsoil	0.13	0.04	CaCO3 % topsoil	0.1	0
silt% subsoil	17	38.9	N % subsoil	0.02	0.03	CaCO3 % subsoil	0.5	0
clay % topsoil	24.9	20.6	CEC topsoil	10.4	13	BD topsoil	1.2	1.5
clay % subsoil	27	20.3	CEC subsoil	8	11	BD subsoil	1.5	1.4
pH water topsoil	7.1	6.6						
pH water subsoil	7.2	6.8						

Note: Soil pH is reaction is an indication of the acidity; OC is organic carbon; N is nitrogen; BC is Bulk Density; CEC is Electrical Conductivity; CaCO3 is Calcium carbonate.

4.3.3 Land Cover Characteristics

Arid regions surface water is formed in wadis, and they are a vital source of water in these areas. Areas contains wadis could lead to catastrophic flash floods, on one hand, a threat to many communities and , on the other, major groundwater recharge sources after rainfall events. Population growth, land use, and human settlements in land around wadis increase social and environmental problems because probably planned exploitation is missing, and water management systems in these areas may cause inconvenience. The study land cover data was retrieved from the Food and Agriculture Organization (FAO)

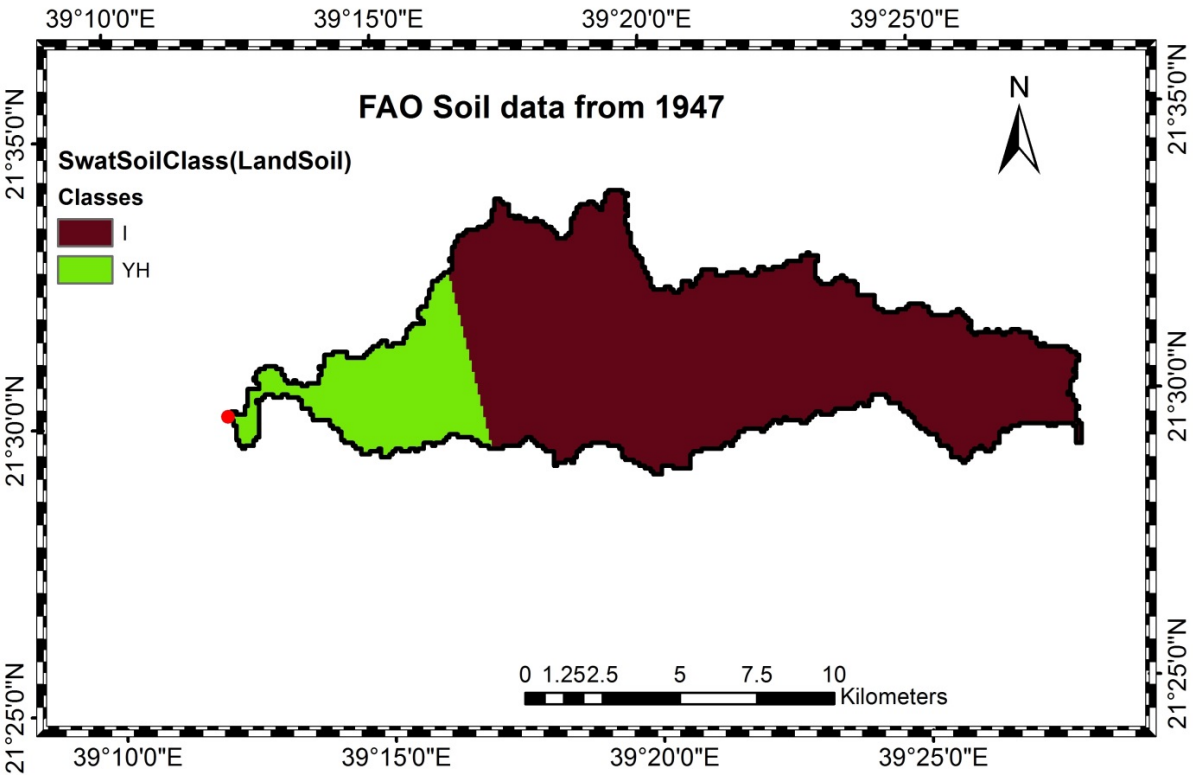

FIGURE 19. Soil cover dataset of 1974 and 1978.

from 2007 dataset with a resolution of five arc minutes. Details and description of Jeddah land cover can be found in TABLE 9 and FIGURE 20. Barren/arid land occupies the largest area in the basin with 35% along with urban area with 23 %. However, vegetation of highland is classified as savanna-wood (Hay). However, a large part of vegetation is composed of mesophytic herbs that only grow following the rain. It is observed that vegetation is denser in highlands than in lower, depressed areas of wadies and closed basins (Nouh 2006). In the western urban area is occupied with high density of residential land.

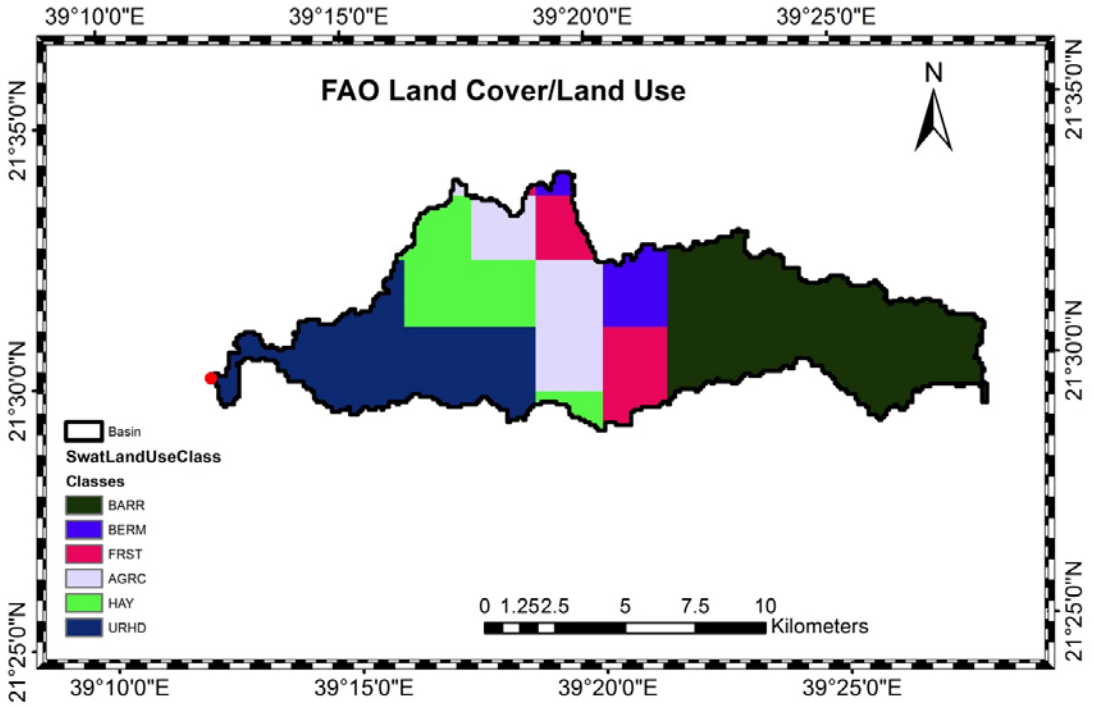

FIGURE 20. Jeddah watershed land cover data set in 2007.

TABLE 9. Summary of the Land Cover/Land Use Characteristics

Land cover/Land use class	Area (Km²)	Percentage Area of total land
Barren land	43.86	35.37
Bermuda Grass	6.74	5.43
Forest	11.04	8.94
Agriculture	16.02	12.92
Hay	17.19	13.87
Urban residential-high density	29.09	23.47

4.3.4 Hydrologic Characteristics

Rainfall distribution is stable from year to year and it is around 100 mm/year. TABLE 10 shows the rainfall stations involved in the study their altitude and location. In FIGURE 7 from CHAPTER 2, this illustrates that most of the rain falls in the winter season (November-January). The four rain stations are surrounding the watershed area. The rainfall stations will be a part of interpolating the values of rainfall in the watershed due to out of boundary location. Climate parameters such as temperature, wind speed, and humidity are also recorded in a daily basis with the same rainfall stations. The runoff record from stream gauges is not available in the basin area.

TABLE 10. Weather Stations Used in the SWAT Model Input

No.	Station Name	Latitude (decimal degrees)	Longitude (decimal degrees)	Elevation(m)
1	Jeddah (KAIA)	21.710	39.187	16.880
2	Makkah	21.438	39.769	240.350

4.4 Results and Discussion

In order to simulate the surface runoff and sediment transportation, SWAT needs a number of climatic data in form of tables such as precipitation, maximum and minimum temperature, relative humidity, and solar radiation. All the data were retrieved, measured, and treated to meet the requirement input of the model. Data source is taken from Presidency of metrological Environment (PME), Global Weather Data for SWAT and the National Climatic Data Center (NCDC).The stations involved into study are located in Jeddah, Yonbu, Medina, and Makkah that captured the climate data shown

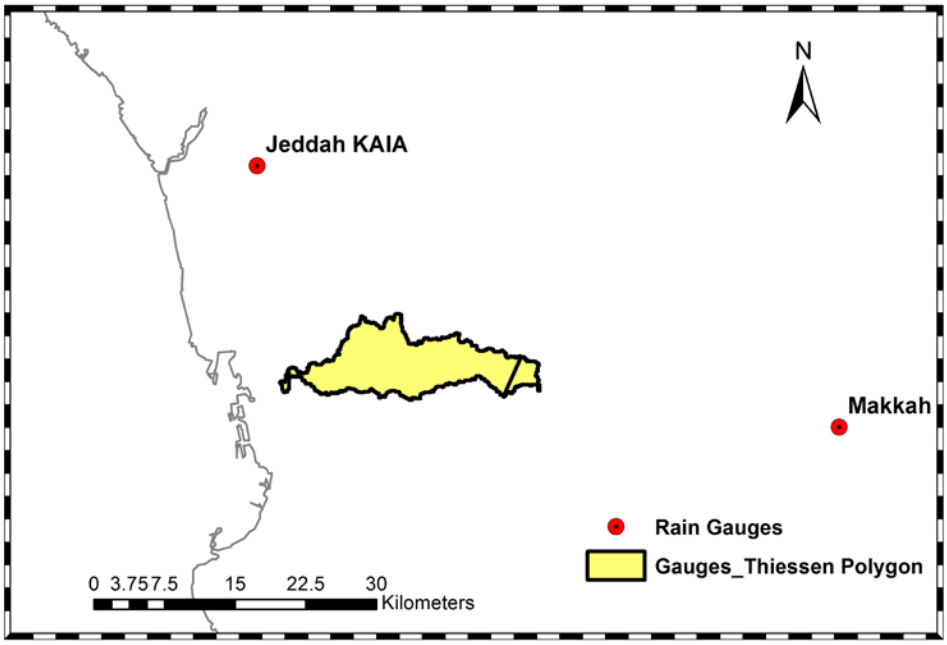

FIGURE 21. Map of weather station locations surrounding the watershed.

in FIGURE 22. The average yearly temperature in the Jeddah watershed lies between 18.6 – 39.9 C°. Average wind speed lies in between 3.1 m/s to 3.9 m/s. Relative humidity in the Jeddah watershed is approximately high to moderate in the range of 50% to 60% due to its location near to the coast. FIGURES 22, 23, 24, and 25 shows the climatological parameters on the region in a daily basis that is affecting the area of study, focusing only on Jeddah station. A summary of monthly climate data gathered from Jeddah station is presented in Table 11, which illustrate the impact of seasonal aspects on the area.

TABLE 11. Summary of the Average Monthly Climate Parameters of Jeddah Station for SWAT Simulation

Month	Temp Max. (°C)	Temp Min. (°C)	Wind (m/s)	Relative Humidity	Solar Radiation (MJ/m²/day)
Jan	29.6	18.6	3.7	0.6	14.9
Feb	30.1	18.9	3.4	0.6	19.9
Mar	32.3	19.7	3.8	0.6	24.3
Apr	34.9	22.2	3.7	0.6	26.0
May	37.5	24.2	3.9	0.5	27.6
Jun	38.8	25.5	3.9	0.6	28.1
Aug	39.5	28.3	3.7	0.6	26.1
Sep	38.0	26.5	3.5	0.6	24.5
Oct	37.3	24.2	2.7	0.6	21.5
Nov	33.9	22.2	3.1	0.6	17.7
Dec	31.4	19.9	3.2	0.6	15.3

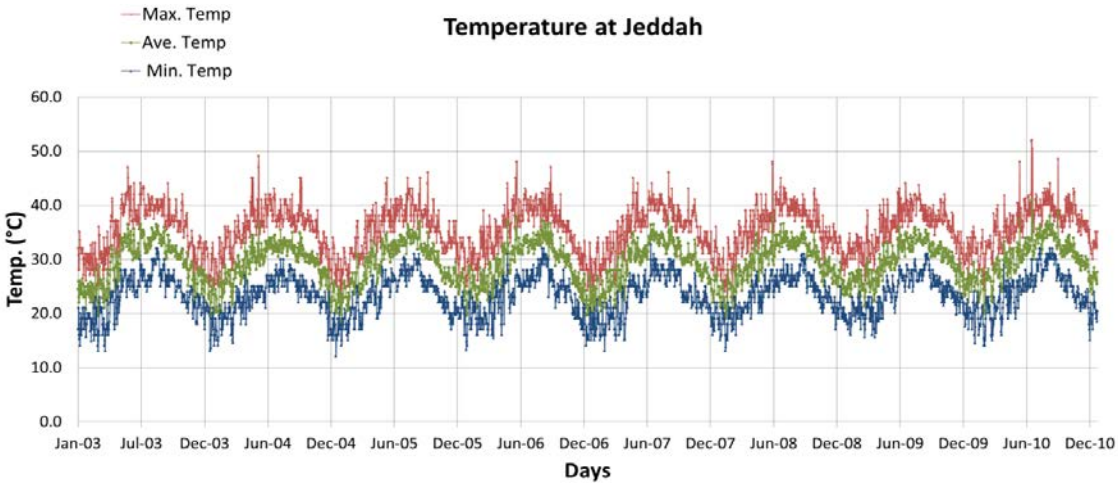

FIGURE 22. Daily average of high and low temperature collected from Jeddah weather station in (C°).

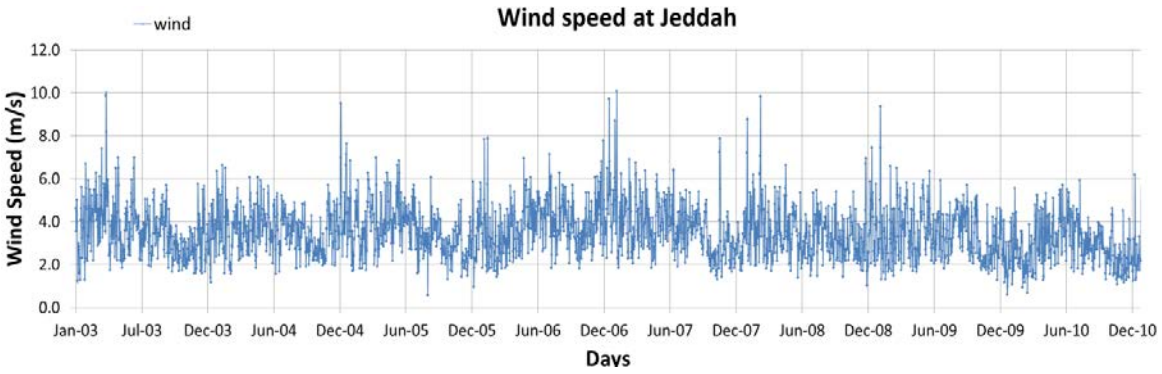

FIGURE 23. Daily wind speed (m/s) got from Jeddah weather station from 2003-2010.

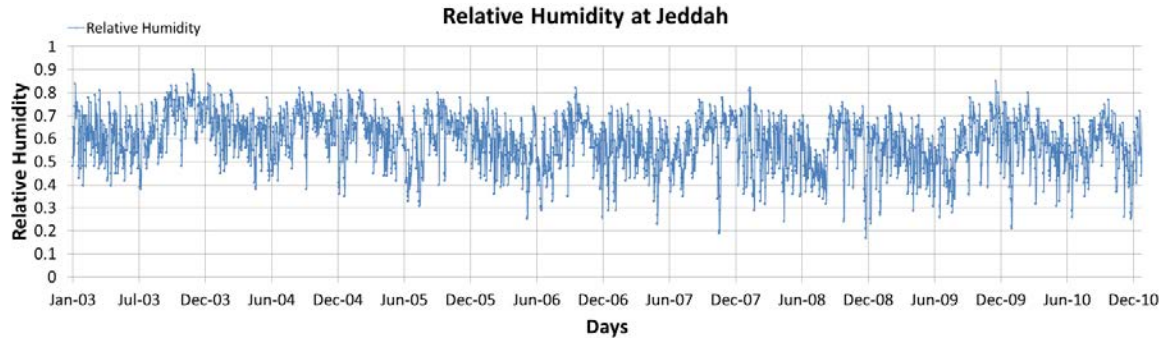

FIGURE 24. Daily relative humidity captured in Jeddah weather station from 2003-2010.

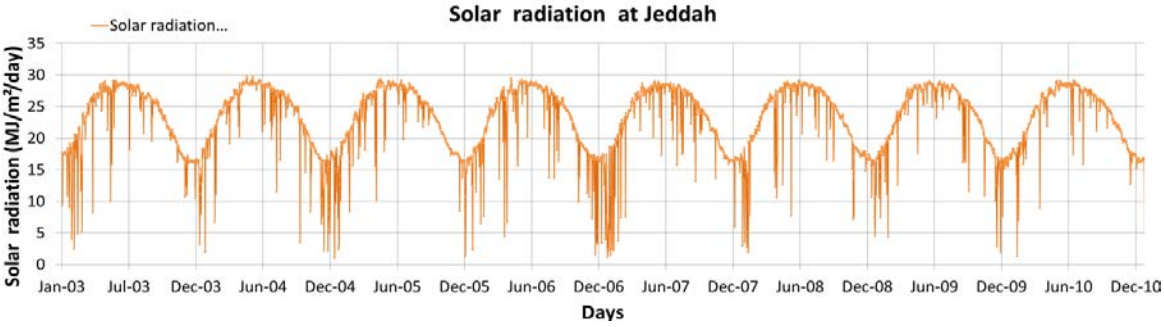

FIGURE 25. Solar radiation recorded in Jeddah weather station from 2003-2010.

4.4.1 Simulations Performance

To better understand the influence of rainfall input on the SWAT model, comparing four rainfall products (TRMM 3b42, PERSIANN, CMORPH, and GSMaP_MVK) that have been used in the same order scenarios. The comparison was performed for the period 2003-2010, according to SWAT simulation validation period, and for grid locations in FIGURE 26. The study is concerned in highlighting the ability, and performance of rain gauge, and satellite using SWAT model that has the ability of interpolating the ungauged watershed to as accurate that can be validated using different statistical methods. Also, compare the satellite products to the rain gauge observations especially at daily and monthly time basis. The four rainfall sources have significant scale discrepancies, with rain gauge giving the point values and satellite products giving values essentially over an area of 0.25° x 0.25° (TRMM 3b42, PERSIANN, and CMORPH) and 0.1° x 0.1° (GSMaP_MVK). The comparison was based on the rainfall grids in FIGURE 26, 27, 28 and 29.

In TABLE 12, the comparison statistics shows the daily correlation as score range of assessing the performance of TRMM 3b42, PERSIANN, CMORPH, and GSMaP_MVK. In the MBE test TRMM and GSMaP_MVK was in good estimate at 0.23 on the other hand PERSIANN estimates were generally agreeing well with the simulated rain gauge observations. NS and CP both products were poorly behaving in performance and prediction skill at a daily basis that is noticeable in PERSIANN and GSMaP_MVK. However, in TABLE 13 monthly basis, all products showed a huge improvement in correlation, performance, and agreement but TRMM 3b42 showed its superiority over PERSIANN, CMORPH, and GSMaP_MVK results. TRMM 3b42 showed high value on

correlation with R= 1 while PERSIANN, CMORPH and GSMaP_MVK showed less correlation with R= 0.23, R= 0.48 and 0.38. TRMM 3b42 and PERSIANN products showed the same almost the MBE outcome as perfect based on Moriasi et al, 2007 relative scale. Based on the rain gauge versus TRMM 3b42, NS generated better values (NS=1) than PERSIANN (NS= -0.44).This also represented in forecast skill, TRMM 3b42 has perfect skill (CP=1) than PERSIANN in forecasting based on the previous observation value.

TABLE 12. Summary of Daily Simulate Run-Off Using Rain Gauge, TRMM 3b42, PERSIANN, CMORPH and GSMaP_MVK

	Daily				
	Sim. Gauge	Sim. TRMM	Sim. PERSIANN	Sim. CMORPH	Sim. GSMaP_MVK
Mean	0.05	0.07	0.05	0.05	0.13
St. dev.	1.20	1.29	1.04	1.20	3.40
Max	59.40	49.90	37.60	59.40	133.00
Min	0.00	0.00	0.00	0.00	0.00
t calculated		2.24	0.00	0.00	1.46
t (two tail)		1.96	1.96	1.96	1.96
MBE		0.28	0.00	1.03	3.11
R^2		0.23	0.01	0.40	0.23
NS		-0.38	-1.04	-0.96	-11.81
CP		-0.38	-1.04	-0.95	-11.78

4.4.2 Run Off and Sediment Transport Simulation Results

The consideration of potential impact of run-off is highly important for hydrologic applications. To further understanding of the current conditions of run-off influences the SWAT model contribution of examining the study area. This approach of

TABLE 13. Summary of Monthly Simulate Run-Off Using Rain Gauge, TRMM 3b42, PERSIANN, CMORPH and GSMaP_MVK

	Monthly				
	Sim. Gauge	Sim. TRMM	Sim. PERSIANN	Sim. CMORPH	Sim. GSMaP_MVK
Mean	1.61	1.64	1.62	3.86	3.27
St. dev.	6.38	6.45	8.26	20.29	12.64
Max	38.94	38.94	76.15	152.38	98.80
Min	0.00	0.00	0.00	0.00	0.00
t calculated		3.42	1.33	1.78	1.45
t (two tail)		1.96	1.96	1.99	1.99
MBE		0.01	0.00	1.03	2.11
R^2		1.00	0.23	0.48	0.38
NS		1.00	-0.44	-1.11	-10.44
CP		1.00	0.07	-0.36	-5.43

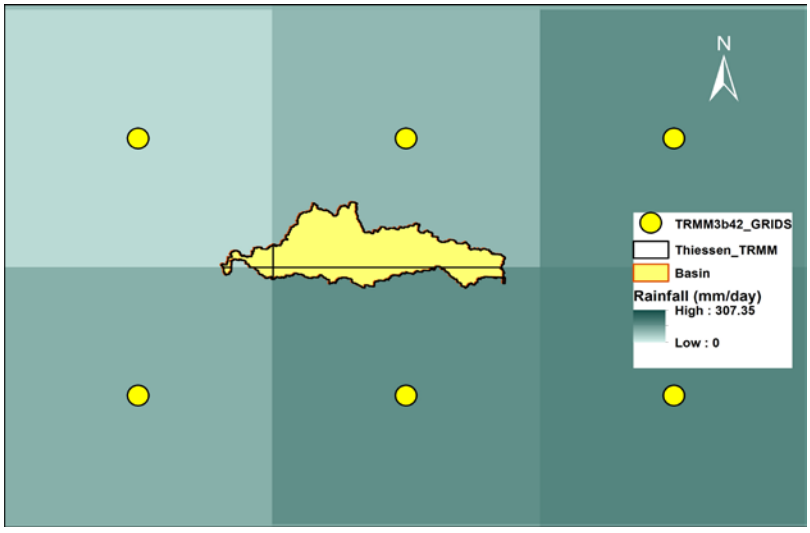

FIGURE 26. Map shown watershed, and 0.25° x0.25°grids of TRMM 3b42 satellite rainfall estimate.

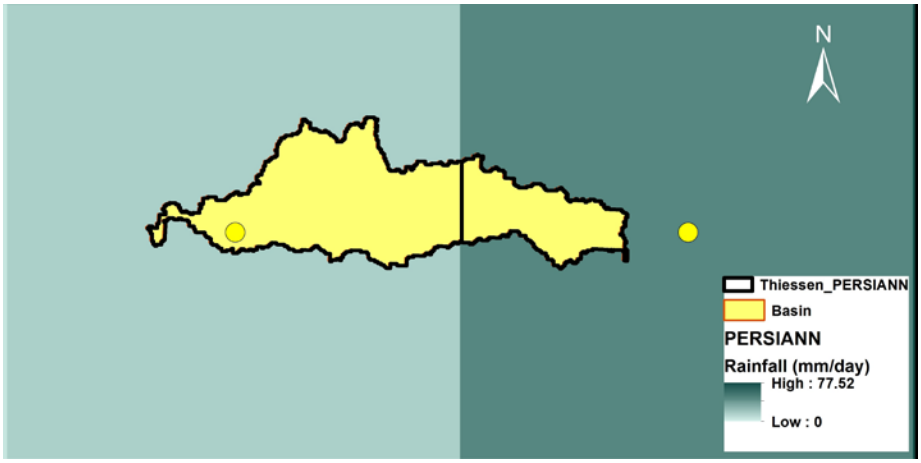

FIGURE 27. Map shown watershed, and 0.25° x0.25°grids of PERSIANN satellite rainfall estimate.

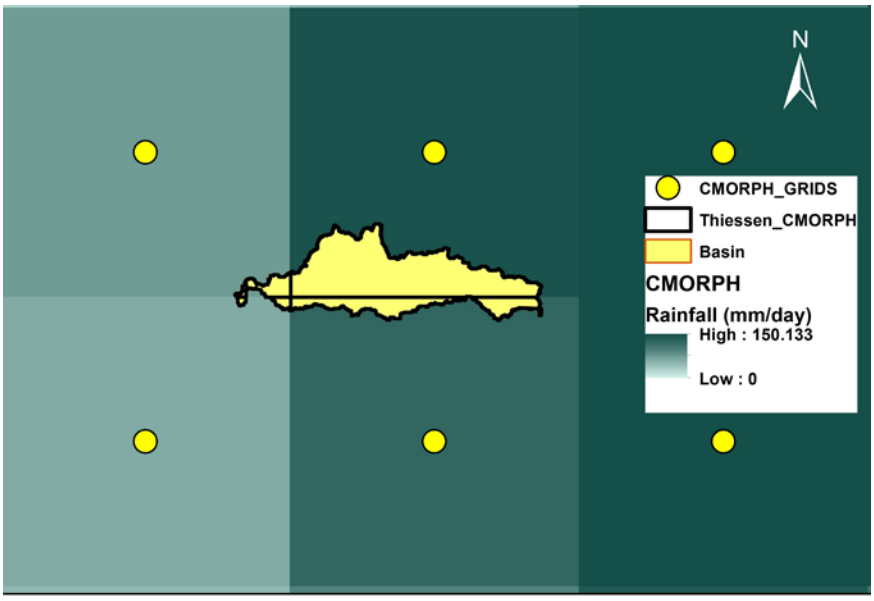

FIGURE 28. Map shown watershed, and 0.25° x0.25°grids of CMORPH satellite rainfall estimate.

FIGURE 29. Map shown watershed, and 0.25° x0.25°grids of GSMaP_MVK satellite rainfall estimate.

modeling shows the difference of performance based on the rain gauge data compared to satellite (TEMM 3b42, PERSIANN, CMORPH, and GSMaP_MVK). Not surprisingly, the better the ground observation, the greater the quality for simulations scenarios. In addition, investigating the sediment transport effect on the area is crucial for flashfloods implications for decision making of designing, developing, and risk analysis for water resources management constructions. In FIGURE 30, monthly evaluation of run off shows that there is no consistency of the rainfall detecting. Mostly in the study area rain peak events were detected with reasonable agreement for November 2003 and November 2009. In 2003, and 2009 extreme events the rain gauge detected 41.7 and 66.1 mm, TRMM 3b42 detecting 0.01 and 63.75mm, PERSIANN under detecting with 4.3 and 35.2 mm, CMORPH over detecting 13.92 and 93.29 mm, and GSMaP_MVK 7.2 and 61.9 mm. In FIGURE 30 illustrates the same behavior of high sediment yield based on the rainfall events that agrees with FIGURE 31. TRMM 3b42 and CMORPH have better agreement with detecting therefore the sediment yield have a slightly higher correlation

than PERSIANN and GSMaP_MVK. In FIGURE 31, it shows the amount of sediment transport on the region that reflects the amount of rainfall. The higher the rainfall amount the higher the run-off as well as sediment transport. In respect to extreme rainfall events in 2003 and 2009 shown in FIGURE 32 and 33 using the Mean Areal Precipitation (MAP) method to calculate the concentrated rainfall that occurred on these two days. Discrepancies of used in simulation satellite products are observed as reflectance of MAP on the run-off results comparing to rain gauge. In 2003 event, all products overestimated and others such as PERSIANN detected rain on a day before the actual rainfall in 11/10/2003 event represented in FIGURE 33. On the other hand, In Nov 25th 2009 TRMM 3b42 showed a huge improvement compared to the 2003 event while GSMaP_MVK had misplaced in time of rainfall event at the same day shown in FIGURE 35.

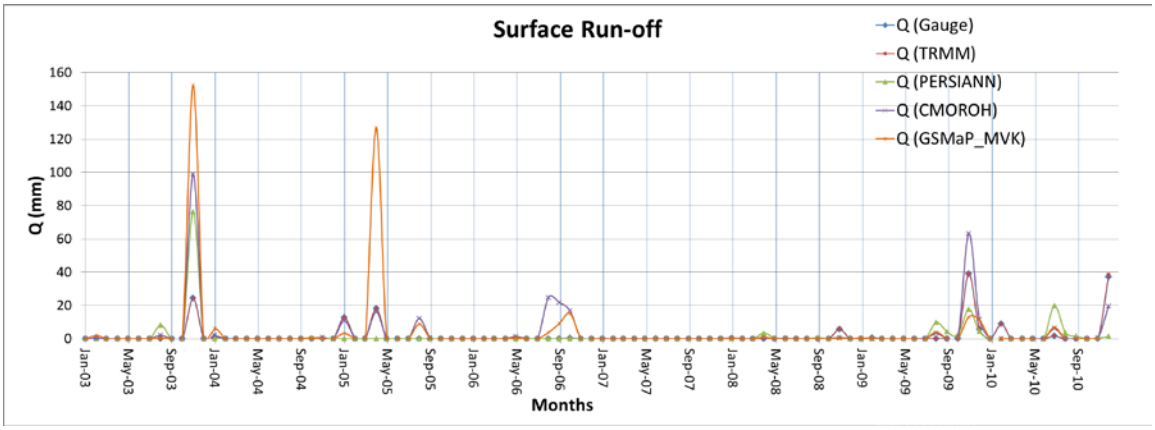

FIGURE 30. Monthly comparison of surface runoff flow of rain gauge, and satellite products (TRMM, PERSIANN, CMORPH, and GSMaP_MVK).

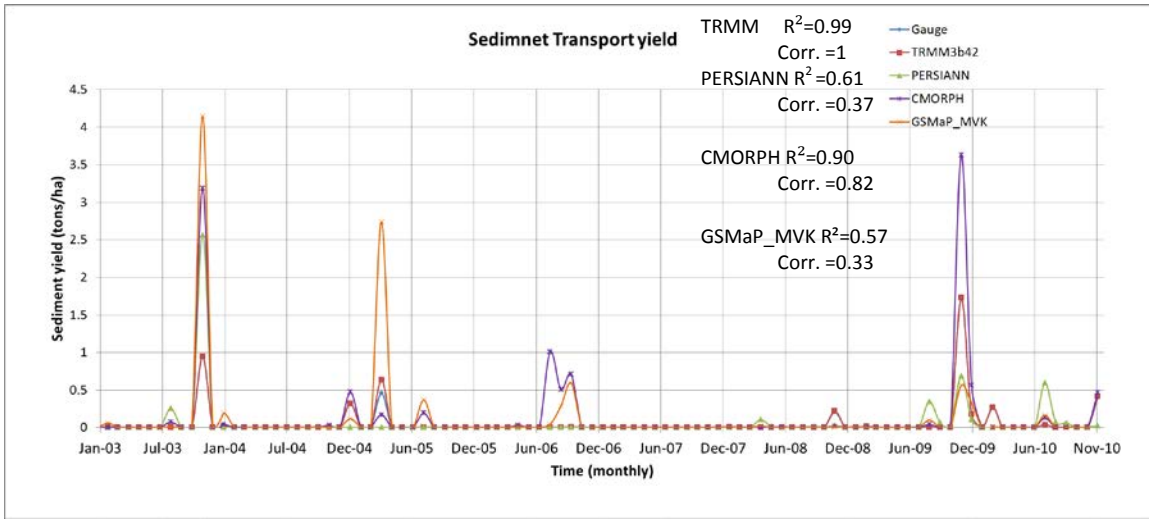

FIGURE 31. Monthly sediment transport over the watershed in (tons/ha) using rain gauge, and satellite products (TRMM, PERSIANN, CMORPH, and GSMaP_MVK).

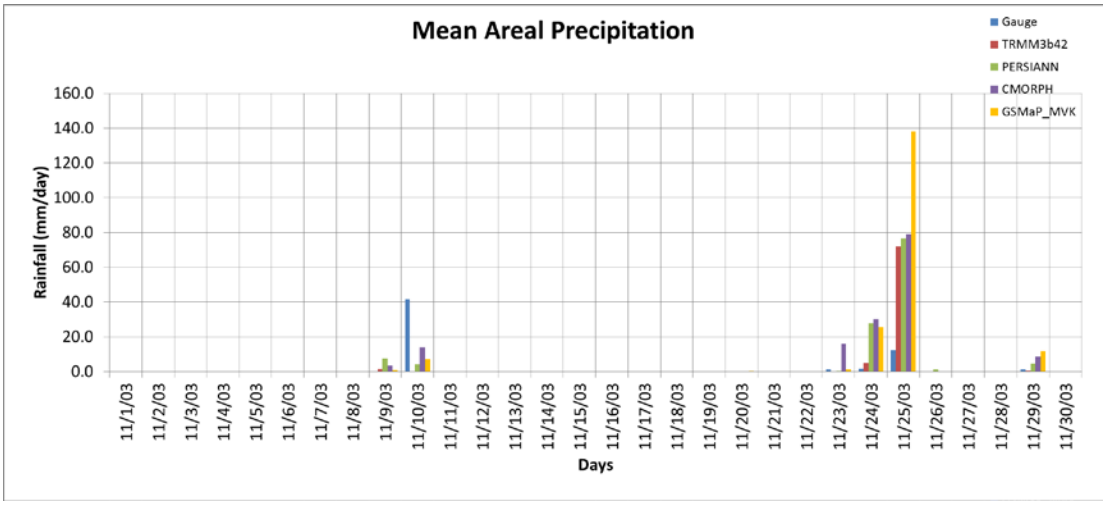

FIGURE 32. Mean areal precipitation for the month of November 2009 event using rain Gauge, TRMM 3b42, PERSIANN, CMORPH, and GSMaP_MVK.

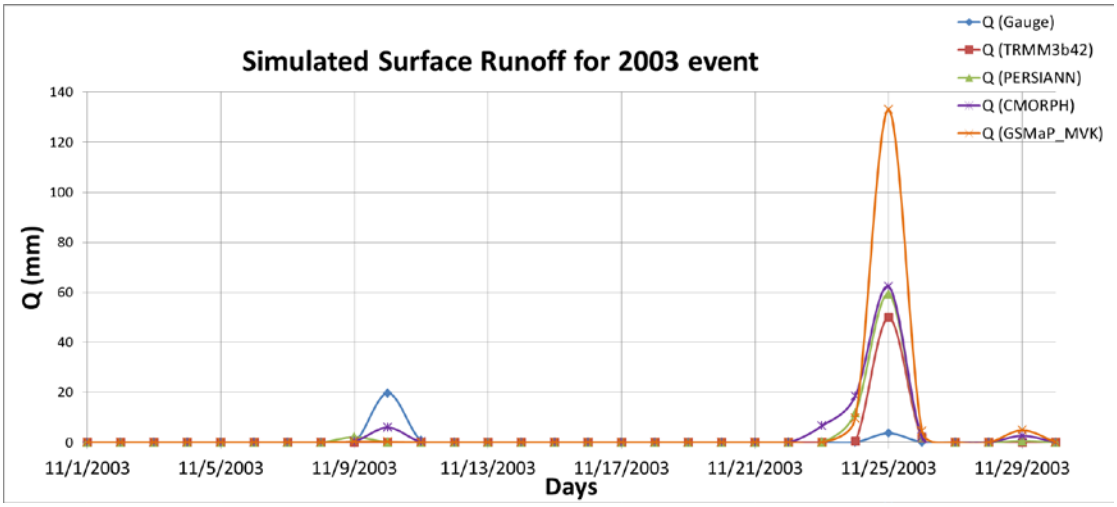

FIGURE 33. Daily comparison of surface runoff flow using rain gauge, and satellite products TRMM 3b42, PERSIANN, CMORPH, and GSMaP_MVK.

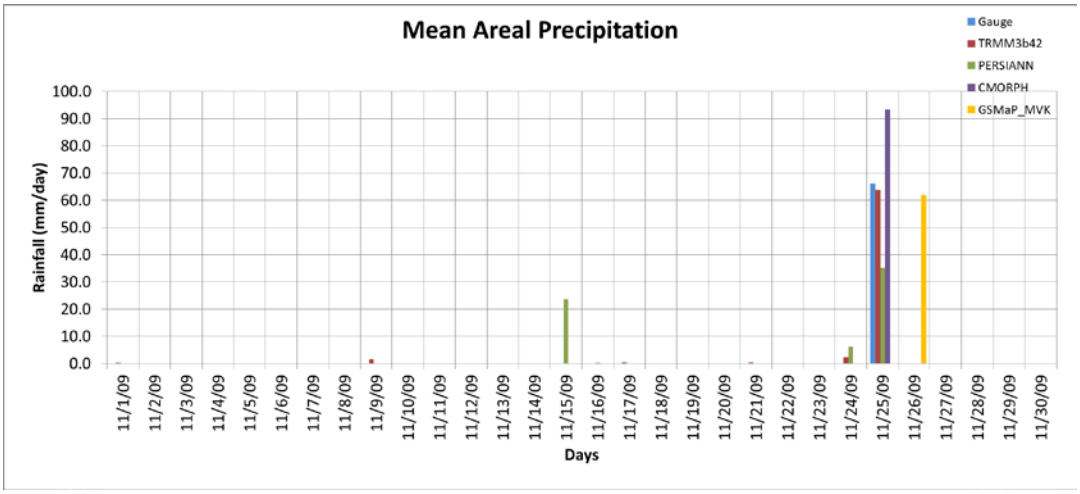

FIGURE 34. Mean areal precipitation for the month of November 2009 event using rain Gauge, TRMM 3b42, PERSIANN, CMORPH, and GSMaP_MVK.

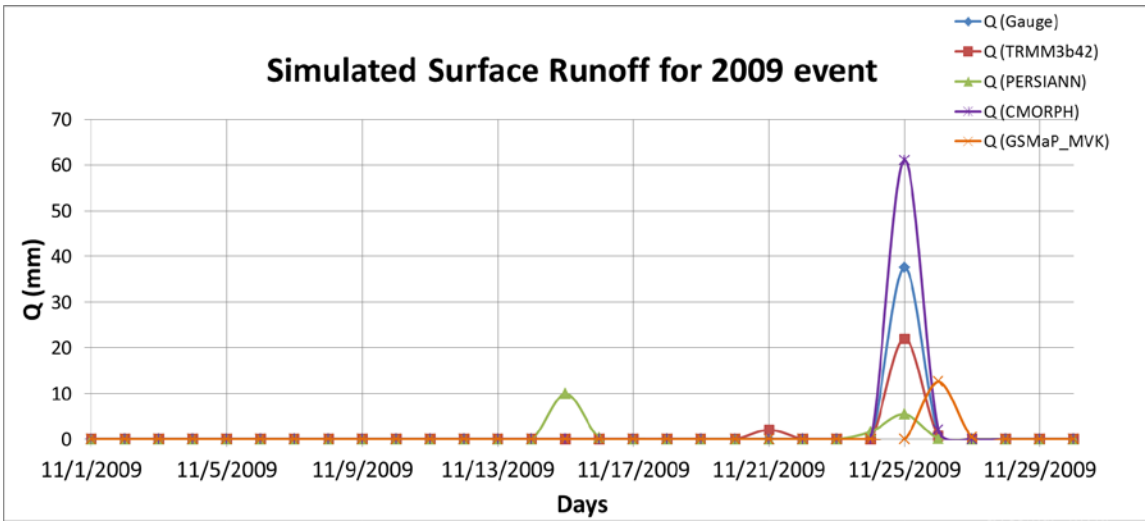

FIGURE 35. Daily comparison of surface runoff flow using rain gauge, and satellite TRMM, and PERSIANN.

4.4.3 Water Balance and Wadi Flow:

SWAT model is a physical algorithm that simulates movement of water, nutrients, and sediments and other hydrologic management within a watershed. SWAT is not a parametric model with a formal optimization procedure (Neitsch et al. 2002). However, variables such as the SCS runoff curve number is assigned with significant degree of uncertainty that could be adjusted to provide better agreeing results. Therefore, a water balance must be checked to ensure better fit. In TABLE 14, an average of rain gauge recordings was assessed to verify the functions of ground water and surface water contribution to the wadi stream.

4.5 Conclusion

The main purpose of the study is to assess the performance of satellite rainfall estimate as an input into hydrological modeling for daily and monthly wadi streamflow simulation in Jeddah, Saudi Arabia. Results from simulation scenarios shows that daily

TABLE 14. Average Monthly Water Balance Result from Rain Gauge Observations

Month	PREC (mm)	ET (mm)	SW (mm)	PC (mm)	SURQ (mm)	LAT_Q (mm)	Total Sim.	% error
Jan	6.33	3.01	0.18	1.31	1.77	0.11	6.39	1.07
Feb	4.00	2.25	0.05	0.61	1.20	0.07	4.19	4.65
Mar	0.00	0.05	0.00	0.00	0.00	0.00	0.05	0.00
Apr	5.81	1.77	0.02	1.64	2.25	0.09	5.78	0.59
May	0.13	0.15	0.00	0.00	0.00	0.03	0.18	45.40
Jun	0.00	0.00	0.00	0.00	0.00	0.00	0.00	0.00
Jul	0.90	0.70	0.00	0.00	0.18	0.02	0.90	0.00
Aug	0.13	0.13	0.00	0.00	0.00	0.00	0.13	0.00
Oct	0.38	0.32	0.02	0.00	0.03	0.00	0.37	0.30
Nov	19.09	4.27	0.60	5.25	8.60	0.37	19.09	0.00
Dec	10.80	2.94	0.58	2.36	5.34	0.15	11.37	5.26

Note. PREC: Total amount of precipitation falling in each month (mm); ET: Actual evapotranspiration from the watershed during the month (mm); SW: Soil water content (mm); PC: Water that percolates past the root zone during the moth (mm); Surface runoff contribution to streamflow during the month (mm); LAT_Q: Lateral flow contribution to streamflow during the month (mm).

satellite products (TRMM 3b42, PERSIANN, CMORPH, and GSMaP_MVK) do not have good agreement with respect to rain gauge observation. In the other hand, switching to monthly basis TRMM 3b42 (R = 1, NS=1, and CP=1) shows better results in regard to relative scales and prediction skills while PERSIANN (R^2= 0.23, NS= -0.44, and CP=0.07) and moderately root mean square result but poorer accuracy in predication for the study period of 2003 to 2010. However, both products TRMM and PERSIANN, MBE comparison have almost the same 0 % value of agreement, which leans toward perfect scale. CMORPH and GSMaP_MVK showed consistent modest skills and in their simulations but over estimation in peak flood events. SWAT model simulates highly depends on spatial rainfall distribution which correspondingly played a major role on daily, and monthly wadi flow rainfall and sediment transport simulations. A high results and better agreement could be reduced if there was better rain gauge network within the watershed especially with daily data.

CHAPTER 5

CONCLUSIONS AND FUTURE DIRECTIONS

5.1 Summary of Findings

Four widely available remotely sensed precipitation satellite products were evaluated over the entire country of Saudi Arabia to study hydrologic response in a semi-arid watershed located at the south west of the country. The four satellite products are TRMM, PERSIANN, CMORPH, and GSMaP_MVK. All the products are available at daily temporal scale but TRMM, PERSIANN, CMORPH rainfall data have coarser (0.25°) gird resolution than GSMaP_MVK (0.1°). Before applying the satellite precipitation data in the model, accuracy of the products was assessed by robust inter-comparison between rain-gauges observations and satellite-retrieved estimates of daily, 10- daily, and monthly rainfall data. Study period for the TRMM, PERSIANN, and CMORPH is January 2003 to December 2011 and for GSMaP_MVK is January 2003 to November 2010.

The products have shown variation in accuracy at different months. Relatively higher correlation between satellite estimates and gauge data during the months of February, August, and October and lower correlation in March, May, September and November for both products, PERSIANN and TRMM. CMORPH and GSMaP_MVK almost have the same pattern of rainfall estimate during the year. Both have a lower correlation in March, June and from September through November a low correlation

value is dominant. However, it is recognizable that higher error is correlated with higher bias values. From the evaluation of the four products for the long-term average of precipitation suggest that TRMM 3B42 offers the best possibility for accurate estimation and variability of precipitation of this high spatial resolution.

The second product PERSIANN aggregated spatially to (0.25°) resolution, accumulated to daily, 10-daily, and monthly totals. PERSIANN monthly events illustrated a poor correlation for all months except for the month of February, which is in the winter season. Statistical method shows that PERSIANN performs poorly in accurately estimating long-term averages.

The evaluation of the third product CMORPH revealed again the superiority of the TRMM 3B42 over the comparison of daily rainfall estimate. In (Table. 5) showing a high overcasting values in the FBS with 1.61 above the perfect score (i.e., 1), and overestimation of the rainfall estimates with a bias value of 1.53. However, the correlation result was balanced with TRMM. In addition, in the HSS CMOPRH scored the highest value of correct to random chance of having a good skill to estimation events. In the 10-daily performance, CMORPH scored significantly high efficiency value as GSMaP_MVK, which show decent prediction performance. In monthly results (Figures 16, a through d), CMORPH showed a dominant underestimation based on the Bias results.

In terms of GSMaP_MVK, the assessment of this product yielded an underestimation throughout the period of the study represented by the highest Bias value of (1.63) daily estimate evaluation (Table5, and Table 6). This product scored high values in POD, MAE, ME which showed a good performance in detecting rainfall events

comparing to TRMM 3B42. In Figures 14, 15, and 17, the balanced estimation is significantly recognizable due to the symmetry of gauge axis. However, GSMaP_MVK and CMORPH both depict reasonably good correlation in the wet season. Eventually, GSMaP_MVK would not perform well in detecting rainfall as TRMM 3B42.

For hydrologic simulation, TRMM, PERSIANN, CMORPH, and GSMa_MVK precipitation products were used as model input. The simulations were compared with the simulated runoff using rain gauge data (called control). All products, TRMM, PERSIANN, CMORPH, and GSMaP_MVK were able to predict the temporal distribution of the two major flood events during the study period. However, all have shown underestimation and overestimation of simulated runoff compared to control.

Results from the validation and hydrologic response are summarized here:

1. The validation analysis of satellite rainfall showed that all the products have good rainfall detection capability at daily time scale. Statistical results for rainfall estimation accuracy show that all the products overestimate rainfall in the region but TRMM 3B42 has less bias, MAE, RMSE than the others.

2. At 10-daily temporal scale, performances of all the products have improved. The products have similar bias as that of daily scale but MAE, RMSE have reduced. TRMM has highest efficiency and PERSIANN has the least among the four products. PERSIANN also show least correlation while the others have more than 50% of correlation with the gauge observation.

3. Statistics at monthly scale show that the accuracy of the products varies in different months. All the products show increased bias and MAE, and decreased efficiency and correlation in the summer time when the region has less rainfall. TRMM

has least bias in the summer while PERSIANN has the highest bias. TRMM also show higher performance in other matrices than other products.

4. However, the products have improved performance in winter season when most of the rain falls. So, all the four satellite products were used for hydrologic evaluation.

5. A 124 km^2 watershed is selected in Jeddah city for hydrologic study. The watershed has semi-arid climate of south-west. The satellite data were used as input in the SWAT hydrologic model. There is no stream gauge in the country and so results from the model with gauge data is considered as "control." The output from satellite precipitation was compared with the truth data and found both CMORPH and TRMM has moderate performance.

6. The study is limited by number of factors. First, for a complete validation of satellite data, it is recommended to have at least 5 observation data within the model grid. However, in the study region there was very scarce observation data and this suggestion could not be considered.

7. There is no stream gauge network in the country and so the model parameters could not be calibrated to increase the accuracy of the simulation of model stream flow.

8. All the products were capable to capture the extreme events of the past decade. Therefore, a regional validation study would have provided further insight satellite rainfall estimation accuracy.

9. TRMM has number of different products available and in this study 3B42 was used. This product is gauge adjusted and so more likely to have a better performance than others. The results also reflect that. However, validation using TRMM real time

(RT) product would have shown if there was indeed any improvement with bias adjusted product.

10. Number of rain gauges is very sparse over the study region, which makes it difficult to conclude from this validation study which satellite product has the best or worst performance. Further, the country experiences two different types of climate- semi arid south west and arid climate in the rest of the region. A validation study over the south-west, where most of the rain falls, could offer more insight on the efficiency of the rainfall products. However, a regionalized validation is very limited in this case because of because of inadequate number of rain gauges over the southwest.

Overall, a major conclusion that can be drawn from this study is that some of the present satellite daily rainfall products are potentially usable in hydrologic response analysis over Saudi Arabia. However, these results indicate there is more room for improvement of these products to remove errors and enhance rainfall estimates.

5.2 Future Directions/Work

Other satellite derived precipitation products will be studied over the study region using conventional statistical methods and new evaluation techniques. A hydrologic model will be simulated using more efficient satellite precipitation product in the southwest part of Saudi Arabia where most of the precipitation falls. The eventual objective is to be able to use a combination of historical gauge and satellite derived rainfall data as inputs to hydrological model (SWAT). In that regard, perhaps the best approach for assessing the satellite rainfall data would be to calibrate the model using historical gauge data and then apply the model using the satellite data. However, simpler and quicker preliminary analyses have been undertaken and are based on pair-wise

comparisons of the gauge data with the satellite data (and in some cases comparisons between gauges in close proximity and between the sources of satellite data). All of the comparisons are based on monthly rainfall totals, as the data are intended for use with monthly time-step hydrological models. The comparisons are based on visual interpretations of the time series of monthly rainfalls, as well as simple statistics Root Mean Square, Bias, and Nash-Sutcliffe efficiency of the best fit linear regression line between the time series pairs. No further statistical measures of fit have been used during this phase of the study, although it is recognized that additional measures may be useful prior to the use of the data within a hydrological model.

The impact of flash flooding on the environment, economy, and society in the region is severe. However, there is no enough investigation on other parts of Saudi Arabia has been examined to reduce the devastating impacts on the region. Consequently, other products should be investigated and validated to find the best fit for the conditions of Saudi Arabia.

REFERENCES

REFERENCES

Abdullah, M. A., and Al-Mazroui, M. A. (1998). "Climatological study of the southwestern region of Saudi Arabia." *I. Rainfall Anal. Climate Res*., 9, 213-223.

AghaKouchak, A., Behrangi, A., Sorooshian, S., Hsu, K., and Amitai, E. (2011). "Evaluation of satellite-retrieved extreme precipitation rates across the central United States." *J. Geophys. Res.*, 115 (D2), doi:10.1029/2010JD014741.

Almazroui, M. (2011). "Sensitivity of a regional climate model on the simulation of high intensity rainfall events over the Arabian peninsula and around Jeddah (Saudi Arabia)." *Theoret. Appl. Climatol.,* 104 (1) , 261-276.

Almazroui, M. A., Al Khalaf, A. K., Abdel Basset, H.M., and Hasanean, H.M. (2009).*Detecting climate change signals in Saudi Arabia using surface temperature,* Project Number (305/428), King Abdelaziz University, Jeddah, Kingdom Of Saudi Arabia.

Benjamin, R. (2011). "Japan's Tsunami and the Internet." Webupon, <http://webupon.com/Web-Talk/Japan's-Tsunami-And-The-Internet/#Ixzz2ce58cwir> (Nov. 2, 2012).

Bitew, M. M., & Gebremichael, M. (2011). "Assessment of satellite rainfall products for streamflow simulation in medium watersheds of the Ethiopian highlands." *Hydrol. Earth Syst. Sci.*, 15(4), 1147-1155.

Bitew, M. M., Gebremichael, M., Ghebremichale, L. T., and Bayissa, Y. A. (2012). "Evaluation of high-resolution satellite rainfall products through streamflow simulation in a hydrological modeling of a small mountainous watershed in Ethiopia." *J. Hydrometeor.,* 13(1), 338-350.

Boushaki, F. I., Hsu, K.-L., Sorooshian, S., Park, G.-H., Mahani, S., and Shi, W. (2009). "Bias adjustment of satellite precipitation estimation using ground-based measurement." *J. Hydrometeor.*, 10(5)1231-1242.

Buda, A., and Jarynowski, A. (2010). *Life-time of correlations and its applications,* Vol. 1, Wydawnictwo Niezalezne, Wroclaw, 5–21.

Dai, A., Trenberth, K. E., and Qian, T. (2004). "A global dataset of Palmer Drought Severity Index for 1870–2002: Relationship with soil moisture and effects of surface warming." *J. Hydrometeor*, 5, 1117–1130.

Dinku, T., Ruiz, F., Connor, S. J., and Ceccato, P. (2009)."Validation and intercomparison of satellite rainfall estimates over Colombia." *J. Appl. Meteorol. Climatol.*, 49, 1004-1014.

Edgell, H. S. (2006). *Arabian deserts: Nature, origin, and evaluation*, Springer, Dordrecht.

Feidas, H., Kokolatos, G., Negri, A., Manyin, M., Chrysoulakis, N., and Kamarianakis, Y. (2009). Validation of an infrared-based satellite algorithm to estimate accumulated rainfall over the Mediterranean basin. *Theoret. Appl. Climatol*., 95 (1-2), 91-109.

Gottschalck, J., Meng, J., Rodell, M., and Houser, P. (2005). "Analysis of multiple precipitation products and preliminary assessment of their impact on global land data assimilation system land surface states." *J. Hydrometeor.*, 6, 573–598.

Hao F., Zhang X., and Yang Z. (2003). *A distributed non-point source pollution model Calibration and validation in Yellow River basin.* Beijing: Institute of Environmental Sciences State Joint Key Laboratory of Environmental Simulation and Pollution Control.

Hasanean, H. M. (2004). *Middle east meteorology,* UNESCO-EOLSS Joint Committee Secretariat, Paris.

Horrocks, K. (2010). "Level 1 and Atmosphere Archive and Distribution System: Land data products." LAADS web. <http://ladsweb.nascom.nasa.gov/data/> (May 1, 2012).

Hsu, K.-L., Gao, X., Sorooshian, S., and Gupta, H. V. (1997). Precipitation estimation from remotely sensed information using artificial neural networks. *J. Appl. Meteorol.*, 36, 1176-1190.

Hsu, K.-L., Gupta, H. V., Gao, X., and Sorooshian, S. (1999). "Estimation of physical variables from multichannel remotely sensed imagery using a neural network: Application to rainfall estimation." *Water Resources Res.,* 35(5), 1605-1618.

Huffman, G. J., Adler, R. F., Bolvin, D. T., Gu, G., Nelkin, E. J., Bowman, K. P., Hong, Y., Erich F. Stocker, E. F., andWolff, D. B. (2007). "The TRMM Multisatellite Precipitation Analysis (TMPA): Quasi-Global, multiyear, combined-sensor precipitation estimates at fine scales." *J. Hydrometeor.*, 8(1), 38-55.

Janowiak, J. E., Joyce, J. R., and Yarosh, Y. (2001). "A real-time global half-hourly pixel-resolution IR dataset and its applications." *Bull. Amer. Meteor. Soc.*, 82, 205–217.

Janowiak, J. E., Xie, P., Joyce, R. J., Chen, M., and Yarosh, Y. (2004, October). "Validation of satellite-derived rainfall estimates and numerical model forecasts of precipitation over the United States." *Proc. 2nd Intl. Precipitation Working Group Workshop,* 25-28 .

Japan Meteorological Agency (2007). "Cp6-precipitation measurements." Japan Meteorological Agency, <http://www.jma.go.jp/jma/jma-eng/jma-center /ric/material/1_lecture_notes/Cp6-Precipitation.Pdf.> (Nov. 2012).

Joyce, R. J., Janowiak, J. E., Arkin, P. A., and Xie, P. (2004). "CMORPH: A method that produces global precipitation estimates from passive microwave and infrared data at high spatial and temporal resolution." *J. Hydrometeor.*, 5, 487-503.

Koppen, W., and Geiger, R. (1928). *Klima der Erde,* Walter de Gruyter, Berlin..

Kozuchowski, K. M. (1993). "Variations of Hemispheric Zonal Index since 1899 and its relationships with air temperature." *Int. J. Climatol.*, 13, 853–864.

Kubota, T., Shige, S., Hashizume, H., Aonashi, K., Takahashi, N., Seto, S., Hirose, M., Takayabu, Y. N., Nakagawa, K., Iwanami, K., Ushio, T., Kachi, M, and Okamoto, K. (2007)."Global precipitation map using satelliteborne microwave radiometers by the GSMaP project." *IEEE Trans.Geosci. Remote Sens*., 45, 2259-2275.

Kummerow, C., Hong, Y., Olson, W. S., Yang, S., Adler, R. F., McCollum, J., Ferraro, R., Petty, G., Shin, D.-B., and Wilheit, T. T. (2001). "The evolution of the Goddard Profiling Algorithm (GPROF) for rainfall estimation from passive microwave sensors." *J. Appl. Meteor*., 40, 1801-1820.

Liss, A. (2011). "Crisis mode: How cultural differences can shape perception." Business insider. <http://www.businessinsider.com/America-is-too-critical-of-Japans-tsunami-and-nuclear-response-2011-6#Ixzz2br48i6kk> (Nov. 3, 2012).

Mckee, T. B., Doesken, N. J., and Kleist, J. (1993). "The relationship of drought frequency and duration to time scales." *Proc. 8th Conf. Applied Climatology*, Anaheim, CA, 179-184.

Ministry of Agriculture and Water (of Saudi Arabia). (1984). *Water atlas of Saudi Arabia*. Riyadh: Ministry of Agriculture and Water.

Moore, E. (1986) *Gardening in the Middle East*, Stacey International, London.

Mosolgo, E., and Dubin, T. (2009) "Summary of HSPF modeling reports in Southern California, Project Number 133904." In: Brown and Caldwell (Ed.), *Hydromodification management plan*, Hydromodification Technical Advisory Committee, San Diego, Appendix C.

Muller, M. J. (1982). *Selected climatic data for a global set of standard stations for vegetation science*, Vol. 5 of *Tasks for vegetation sciences*, Kluwer Academic Publishers Group, Dordrecht..

Nash, J. E., and Sutcliffe, J. V. (1970). "River flow forecasting through conceptual models: Part I—A discussion of principles." *J. Hydrol.*, 10(3), 282–290.

National Climatic Data Center. (2012, May 4). "U.S. standardized precipitation index." <http://lwf.ncdc.noaa.gov/oa/climate/research/prelim/drought/spi.html> (April 1, 2012).

Neitsch, S. L., Arnold, J. G., and Srinivasan, R. (2002). *Pesticides fate and transport predicted by the Soil And Water Assessment Tool (SWAT)*, Grassland, Soil And Water Research Service, Temple, TX, <http://www. brc. tamus. edu/swat /applications/sugarcreekin. pdf> (Nov. 2012).

Nouh, M. (2006). "Wadi flow in the Arabian Gulf states." *Hydrolog. Proc.*, 20 (11), 2393-2413.

Novella, N., and Thiaw, W. (2008). *Validation of satellite-derived rainfall products over the Sahel.* Camp Springs, MD: Wyle Information Systems, National Oceanic and Atmospheric Administration, Climate Prediction Center, 1-10.

Nurmi, P. (2003, December). *Recommendations on the verification of local weather forecasts operations,* ECMWF Technical Memoranda. Helsinki: Finnish: Meteorological Institute.

Okamoto, K., Iguchi, T., Takahashi, N., Ushio,T., Awaka, J., Shige, S., and Kubota, T. (2007). "High precision and high resolution global precipitation map from satellite data." *Proc. Intl. Symp. Antennas and Propagation, ISAP*, 506-509.

Singh, V., and Frevert, D. (2002). *Mathematical models of small watershedd hydrology and applications*, Water Resources Publications, Highlands, CO.

Singh, J., Knapp, H. V., and Demissie, M. (2005) "Hydrologic modeling of the Iroquois River watershed." *JAWRA: J. Am. Water Resources Assoc.,* 41(2), 343-360.

Sohn, B. J., Han, H.-J., and Seo, E.-K. (2010). "Validation of satellite-based high-resolution rainfall products over the Korean peninsula using data from a dense rain gauge network." *J. Appl. Meteor. Climatol.*, 49, 701–714.

Sorooshian, Soroosh, Hsu, K.-L., Gao, X., Gupta, H. V., Imam, B., and Braithwaite, D. (2000). "Evaluation of PERSIANN system satellite-based estimates of tropical rainfall." *Bull. Am. Meteor. Soc.*, 81(9), 2035-2046.

Stampoulis, D., and Anagnostou, E. N. (2012). "Evaluation of global satellite rainfall products over continental Europe." *J. Hydrometeor.*, 13, 588–603.

Subyani, A. M. (2004). "Geostatistical study of annual and seasonal mean rainfall patterns in southwest Saudi Arabia." *Hydrol Sci.*, 49, 803–817.

Subyani, A. M. (2011). "Hydrologic behavior and flood probability for selected arid basins in Makkah area, western Saudi Arabia." *Arab. J. Geosci.*, 4(5-6), 817-824.

Subyani, A. M., Al-Modayan, A. A., and Al-Ahmadi, F. S. (2010). Topographic, seasonal and aridity influences on rainfall variability in western Saudi Arabia. *J. Environ. Hydrol.*, 18, paper 2.

Thiemig, V., Rojas, R., Zambrano-Bigiarini, M., Levizzani, V., and De Roo, A. (2012). "Validation of satellite-based precipitation products over sparsely gauged African river basins." *J. Hydrometeor.*, 13, 1760–1783.

Tobin, K. J., and Bennett, M. E. (2012). "Validation of satellite precipitation adjustment methodology from seven basins in the continental United States." *JAWRA: J. Am. Water Resources Assoc.*, 48(2), 221-234.

Walter, H., and Lieth, H. (1960). *Klimadiagramm-weltatlas,* Gustav Fischer Verlag, Jena.

Washington, R., Todd, M., Middleton, N.J., and Goudie, A.S.(2003). "Dust-storm source areas determined by the total ozone monitoring spectrometer and surface observation." *Ann. Assoc. Am. Geographers,* 93, 297-313.

Wikipedia. (2013). "Geography of Saudi Arabia." Wikipedia < http://en.wikipedia.org /wiki/Geography_of_Saudi_Arabia> (August 2013).

Wikipedia. (2013). "Hijaz mountains." Wikipedia <http::en.wikipedia.org/wiki/Hijaz _mountains> (August 2013).

Wikipedia. (2013). "Saudi Arabia: Geography." Wikipedia <http://en.wikipedia.org/wiki /Saudi_Arabia#Geography> (August 2013).

Wilheit, T. T. (1986). "Some comments on passive microwave measurements of rain." *Bull. Amer. Met. Soc.*, 67, L226-232.

Yan, J., and Zhang, J. (2001). *Evaluation of the MIKE SHE modeling system,* Southern Cooperative Series Bulletin 398, Raleigh, NC: Southern Association of Agricultural Experiment Station Directors.

Zhao, F., and Shepherd, M. (2012)."Precipitation changes near Three Gorges Dam, China." *J. Hydrometeor*:, 13, 735-741.